

## TABLE OF CONTENTS

1. Introduction and Objectives.....	1
1.1 Introduction .....	7
1.2 Objectives.....	7
1.3 Outline of the thesis.....	8
1.4 Impact of COVID 19 on this study .....	8
2. Historic Literature review .....	9
2.1 Baroque – Architectural Style.....	10
2.2 Churches in Broumov region .....	10
2.2.1 Introduction .....	10
2.2.2 Broumov Group of Churches:.....	10
3. State of the art review .....	13
3.1 Material – Sandstone .....	13
3.1.1 Applicability of review .....	15
3.2 Masonry modeling strategies using finite element method .....	15
3.2.1 Detailed Micro-modeling.....	16
3.2.2 Macro-modeling.....	16
3.2.3 Homogenization techniques .....	17
3.2.4 Applicability of review .....	17
3.3 Material Constitutive Model.....	18
3.3.1 Applicability of review .....	18
3.4 Discretization using finite element method.....	19
3.4.1 Applicability of review .....	19
4. Experimental test procedures.....	21
4.1 Determination of Compressive strength in accordance with BS EN 1052-1:1999.....	21
4.2 Diagonal Compression Test in accordance with ASTM E519-02 .....	22
4.3 Measurement of in-plane shear strength of masonry mortar joint in accordance with ASTM C1531-02.....	23
5. Numerical Analysis.....	25
5.1 Wall Topology and Model Geometry.....	25
5.2 Masonry Arrangement and MQI .....	28
5.2.1 Vertical Loading.....	29

5.2.2	In-plane Loading .....	30
5.2.3	Evaluation of strength parameters using MQI .....	31
5.3	Material Properties and Constitutive material model .....	32
5.4	Numerical Model .....	34
5.4.1	Compression Test .....	34
5.4.2	Tension Test .....	35
5.4.3	In-plane Shear Test .....	35
6.	Results .....	37
6.1	Compression Test .....	37
6.2	Tension Test .....	38
6.3	Shear Test .....	39
7.	Discussion .....	41
7.1	Compression Test .....	41
7.2	Tension Test .....	41
7.3	Shear Test .....	42
7.4	Validation of Results .....	42
8.	Conclusion and future recommendations .....	45
9.	References .....	47
10.	Appendix A .....	49
11.	Appendix B .....	61

## LIST OF FIGURES

Figure 2.1 – Geographic map of Czech Republic .....	9
Figure 2.2 – Locations of Broumov churches marked on google maps .....	11
Figure 3.1 – Božanov Sandstone .....	13
Figure 3.2 – Dubenec Sandstone.....	13
Figure 3.3 – Havlovice Sandstone .....	13
Figure 3.4 – Havlovice Sandstone .....	14
Figure 3.5 – Kocbeře Sandstone.....	14
Figure 3.6 – Kocbeře Sandstone.....	14
Figure 3.7 – Hořice Sandstone.....	14
Figure 3.8 – Trutnov Sandstone.....	15
Figure 3.9 – Záměl Sandstone .....	15
Figure 3.10 – Masonry assembly and Modelling types (11) .....	16
Figure 3.11 – Micromodel possible failure mechanisms (12).....	16
Figure 3.11 – Micro to macro-level through homogenization.....	17
Figure 4.1 – Experimental test setups - Compression test (left), diagonal compression test (middle), in-plane shear test (right) .....	21
Figure 5.1- As-built wall assembly 1 (left), Atena 2D model configuration (right) .....	26
Figure 5.2- As-built wall assembly 2 (left), Atena 2D model configuration (right) .....	26
Figure 5.3- As-built wall assembly 3 (left), Atena 2D model configuration (right) .....	27
Figure 5.4- As-built wall assembly 4 (left), Atena 2D model configuration (right) .....	27
Figure 5.5– Correlation curves: MQI values vs compressive strength.....	31
Figure 5.6– Correlation curves: MQI values vs shear strength.....	31
Figure 5.7– Correlation curves: MQI values vs Young's modulus of elasticity .....	32
Figure 5.9– Uni-axial stress-strain law (left), Biaxial failure function (right) (15).....	33
Figure 5.10– Exponential crack opening law in tension. Stress- crack width diagram (left), Compressive stress-strain diagram (middle) Exponential crack opening law in shear. Stress- crack width diagram (right).....	33
Figure A1– Church of St Jakub Větší in Ruprechtice.....	51
Figure A2– Church of St. George and Martin in Martínkovice .....	52
Figure A3– Church of St. Anne in Vižňov.....	53
Figure A4– Church of St. Michal in Verněřovice .....	54
Figure A5– Church of All Saints in Heřmánkovice .....	55
Figure A6– Church of All Saints in Heřmánkovice .....	56
Figure A7– Church of St. Barbora in Otovice.....	57

Figure A8– Church of St. St. Margaret in Šonov .....	58
Figure A9– Church of St. Mary Magdalene in Božanov .....	59
Figure B1 - Max Principal Stress (left), legend (right) .....	63
Figure B2 – crack width (left), legend (right).....	63
Figure. B3 - Principal plastic strain X (left), legend (right) .....	63
Figure. B4 - Principal plastic strain Y (left), legend (right) .....	63
Figure B5 - Max Principal Stress (left), legend (right) .....	64
Figure B6 – crack width (left), legend (right).....	64
Figure B7- Principal plastic strain X (left), legend (right) .....	64
Figure B8 - Principal plastic strain Y (left), legend (right) .....	64
Figure B9 - Max Principal Stress (left), legend (right) .....	65
Figure B10 – crack width (left), legend (right) .....	65
Figure B11 - Principal plastic strain X (left), legend (right) .....	65
Figure. B12 - Principal plastic strain Y (left), legend (right) .....	65
Figure. B13 - Max Principal Stress (left), legend (right) .....	66
Figure B14 – crack width (left), legend (right) .....	66
Figure B15 - Principal plastic strain X (left), legend (right) .....	66
Figure B16 - Principal plastic strain Y (left), legend (right) .....	66
Figure B17 - Max Principal Stress (left), legend (right) .....	67
Figure B18 – crack width (left), legend (right) .....	67
Figure B19 - Principal plastic strain X (left), legend (right) .....	67
Figure B20 - Principal plastic strain Y (left), legend (right) .....	67
Figure B21 - Displacement Y (left), legend (right) .....	67
Figure B22 – Tensile strength (left), legend (right) .....	67
Figure. B23 - Max Principal Stress (left), legend (right) .....	68
Figure B24 – crack width (left), legend (right) .....	68
Figure B25 - Principal plastic strain X (left), legend (right) .....	68
Figure B26 - Principal plastic strain Y (left), legend(right) .....	68
Figure B27 - Displacement Y (left), legend (right) .....	68
Figure B28 – Tensile strength (left), legend (right) .....	68
Figure B29 - Max Principal Stress (left), legend (right) .....	69
Figure B30 – crack width (left), legend (right) .....	69
Figure. B31 - Principal plastic strain X (left), legend (right) .....	69
Figure B32 - Principal plastic strain Y (left), legend (right) .....	69
Figure B33 - Displacement Y (left), legend (right) .....	69
Figure B34 – Tensile strength (left), legend (right) .....	69
Figure B35 - Max Principal Stress (left), legend (right) .....	70
Figure B36 – crack width (left), legend (right) .....	70

Figure B37 - Principal plastic strain X (left), legend (right).....	70
Figure B38 - Principal plastic strain Y (left), legend (right).....	70
Figure B39 - Displacement Y (left), legend (right).....	70
Figure B40 – Tensile strength (left), legend (right).....	70
Figure B41 - Max Principal Stress (left), legend (right) .....	71
Figure B42 – crack width (left), legend (right) .....	71
Figure B43 - Principal plastic strain X (left), legend (right).....	71
Figure B44 - Principal plastic strain Y (left), legend (right).....	71
Figure B45 - Displacement X (left), legend (right).....	71
Figure B46 - Max Principal Stress (left), legend (right) .....	72
Figure B47 – crack width (left), legend (right) .....	72
Figure B48 - Principal plastic strain X (left), legend (right).....	72
Figure B49 - Principal plastic strain Y (left), legend (right).....	72
Figure B50 - Displacement X (left), legend (right).....	72
Figure B51 - Max Principal Stress (left), legend (right) .....	73
Figure B52 – crack width (left), legend (right) .....	73
Figure B53 - Principal plastic strain X (left), legend (right).....	73
Figure B54 - Principal plastic strain Y (left), legend (right).....	73
Figure B55 - Displacement X (left), legend (right).....	73
Figure B56 - Max Principal Stress (left), legend (right) .....	74
Figure B57 – crack width (left), legend (right) .....	74
Figure B58 - Principal plastic strain X (left), legend (right).....	74
Figure B59 - Principal plastic strain Y (left), legend(right).....	74
Figure B60 - Displacement X (left), legend (right).....	74

## LIST OF TABLES

Table 3.1 – Characteristics of locally found sandstone in the region of Královéhradecký.....	15
Table 3.2 – Atena user's manual Part 2-1 Table 4-1 (14).....	19
Table 5.1– Wall assembly model information .....	25
Table 5.2– Classification of masonry according to method of MQI (19) .....	28
Table 5.3– Calculation of MQI Parameters under vertical loading – Wall assembly 1 (Left), Wall assembly 2 (Right) .....	29
Table 5.4– Calculation of MQI Parameters under vertical loading – Wall assembly 3 (Left), Wall assembly 4 (Right) .....	29
Table 5.5– Calculation of MQI and quality of the masonry .....	29
Table 5.6– Calculation of MQI Parameters under lateral loading – Wall assembly 1 (Left), Wall assembly 2 (Right) .....	30

Table 5.7– Calculation of MQI Parameters under vertical loading – Wall assembly 3 (Left), Wall assembly 4 (Right) .....	30
Table 5.8– Calculation of MQI and quality of the masonry.....	30
Table 5.9– Estimations of strength parameters of masonry wall assemblies using MQI method.....	32
Table 5.10– Summary of material properties obtained from past studies (20, 21) .....	34
Table 6.1 – Comparison between Compressive Stress and Strain values of wall assemblies.....	37
Table 6.2 – Standard deviation, average, and Coefficient of variation between wall assemblies 1 through 4.....	37
Table 6.3 – Comparison between Compressive Stress and Strain values of wall assemblies.....	38
Table 6.4 – Standard deviation, average, and Coefficient of variation between wall assemblies 1 through 4.....	38
Table 6.5– Comparison between Compressive Stress and Strain values of wall assemblies.....	39
Table 6.6 – Standard deviation, average, and Coefficient of variation between wall assemblies 1 through 4.....	39
Table 6.7 – Standard deviation, average, and Coefficient of variation between wall assemblies 2 through 4.....	39
Table 7.1– Comparison between strength parameters of wall assemblies.....	42
Table 7.2– Comparison between average compressive strength of wall assemblies and recommended values from NTC 2018 and 2019 commentary.....	43
Table 7.3– Comparison between average shear strength of wall assemblies and recommended values from NTC 2018 and 2019 commentary .....	43
Table 8.1– Comparison between strength parameters of wall assemblies.....	45

## LIST OF GRAPHS

Graph 6.1– Comparison between Compressive Stress vs Strain curves .....	37
Graph 6.2– Comparison between Tensile Stress vs Strain curves.....	38
Graph 6.3– Comparison between Shear Stress vs Strain curves.....	39

## **1. INTRODUCTION AND OBJECTIVES**

### **1.1 Introduction**

Stone Masonry is one of the oldest construction materials used around the world due to the availability of raw material locally, easy manufacturing processes, and simple construction technique. Historic masonry did survive the test of time and is still relevant as a material that works best in compression (strong and durable) with very low tensile strength.

In the early days, before the development of the transportation system, locally found stone (granite sandstone limestone, etc.) was collected and used the way it was found by laying stone units on top of one another using dry joints. Through years with experience, builders and specialists realized the need for dimensional stone, stone quarries, and use of binding materials between two stones for better performance, longer spans, and taller structures.

Structural masonry walls in any load-bearing structure are normally subjected to compressive stresses due to gravity loading. But compression can lead to units also subject to tensile stresses since mortar/binding material has much lower stiffness than that of units(1). Up to a certain extent, the exterior wall system also helps to resist and transfer in-plane lateral loads generated by seismic or wind actions when box behavior is achieved.

In recent years, vast improvements and progress were achieved in research and design building code development of the use of structural steel and reinforced and pre-stressed concrete as a modern building material with moment frame structural system. This trend led to stone/brick masonry mostly being used as a nonstructural infill material of reinforced concrete frames which directly impacted improvements and research on the use of structural stone masonry and now there is no national/EU reference standard/building code for stone masonry.

Nevertheless, conservation and strengthening of built heritage are essential to protect the historic significance and avoid structural damage, reduction in strength, and possible collapse. This requires the identification of deficiencies and possible damage mechanisms of existing structures and appropriate intervention solutions.

### **1.2 Objectives**

The main objective of this study is to calculate and evaluate the strength of the walls of different bricklayer's patterns of broumov churches in compression, tension, and shear.

It is very difficult to numerically estimate the strength of irregular masonry with random topology and typology. To determine homogenized properties of masonry walls for full-scale 3D models, micro-

modeling with finite element method approach is conducted in this study to observe the global and local behavior of masonry wall in various applications and loading conditions.

### **1.3 Outline of the thesis**

After the introduction chapter, the thesis is then divided into seven additional chapters.

Chapter 2 presents the literature review of the Czech Republic, Churches of Broumov region, and baroque architecture to familiarize the reader with the history behind the construction of broumov churches and the timeline of construction.

Chapter 3 is associated with the state of the art review of locally obtained stones in the broumov region, and review of necessary concepts and strategies used in the numerical modeling of this study

Chapter 4 goes through a standard testing procedure for experimental tests to obtain the strength parameters of masonry.

Chapter 5 deals with Numerical modeling of wall assemblies loading conditions and nonlinear properties associated with numerical modeling using Finite element analysis.

Chapter 6 captures the results obtained from numerical modeling for loading in compression, tension, and shear

In chapter 7, the numerical results are discussed and strength parameters are then compared directly based on the different stone bricklayer's pattern.

Finally, in chapter 8, an extended summary of results concluding remarks with suggestions for future work are given.

### **1.4 Impact of COVID 19 on this study**

Experimental and Laboratory campaign could not be conducted due to the special circumstances of Pandemic Covid-19 to validate the results from numerical calculations. MQI method and suggested values from NTC 2008 and commentary 2009 were used for validation of strength parameters.



## 2. HISTORIC LITERATURE REVIEW

The country of the Czech Republic is located in Central Europe with an approximate area of 78,866 sq.kms. It shares northern borders with Germany and Poland and southern borders with Austria and Slovakia. It is part of the European Union (EU) since 2004 and part of the Schengen area since 2007 which allows free movement within EU territory. The geographical position of the nation and its well-connected transportation network allowed the city of Prague in the Czech Republic to grow into an international transit hub.



Figure 2.1 – Geographic map of Czech Republic

Evidence of history in today's Czech states can go back up to 25000 years. Historical evidence documented arrival of tribes like Celtic Boii (Bohemia is derived from), Germanic Marcomanni and Quadi in the region during 1<sup>st</sup> century BC. Looking back at the history, following major events built (2) and shaped the fortunes and misfortunes of what we now know as Country of the Czech Republic.

- Arrival of Slavs
- Samo Kingdom
- Unification of Bohemia
- The ruling of King Premyslid to Bohemian throne
- The ruling of King Luxemburg to Bohemian throne
- The ruling of King Hasburg to Bohemian throne

- Thirty-year war during the 17<sup>th</sup> century
- Czechoslovak Declaration of Independence in 1918
- Separation of two countries the Czech Republic and the Slovak Republic

## 2.1 Baroque – Architectural Style

Baroque, a new Architectural Style gave fresh look at how large structures with simple geometric shapes can enhance the character of the building and be a symbol during the 17<sup>th</sup> and 18<sup>th</sup> Centuries. There are 122 world heritage properties cited by UNESCO with Baroque Architecture. (3)

After the victory in the 30-year long war in the 17<sup>th</sup> century, Catholics started rebuilding the nation around the City of Prague with the latest trend of new architectural style – Baroque which means irregular stone in Portuguese. Even though the style originally came from Italy; during the high baroque period, local and German architects played a major role to shape and reinvent the style in Czech lands. Kryštof Dientzenhofer and Kilián Ignác Dientzenhofer, father-son pair were one of the most decorative architects of the time who worked on many great projects.

## 2.2 Churches in Broumov region

### 2.2.1 Introduction

Broumov region in the northeastern part of the Czech Republic is famous for its countryside setting, natural landscapes, and unique rock formations. The presence of Mountains in the region (Javoří Hory Mountains, Table Mountains, and the Jestřebí Hory Mountains), various trails and hikes, huge sandstone formations, mammoth rock towers with country roads in combination with woods and fields situated around the rock towns of adrspach and Teplice allows a region to attract local and foreign tourists.

Broumov region has an area of around 410 sq.kms, with history referencing almost 100 years of human colonization near the broumov basin of river Stenava. The region has rich architecture featuring Baroque Styled Churches and monasteries built in the late 16<sup>th</sup> and early 17<sup>th</sup> centuries. (4)

### 2.2.2 Broumov Group of Churches:

There are nine main churches (built between the late 16<sup>th</sup> and early 17<sup>th</sup> century) in the Broumov region as listed below(5).

- Church of St. George and Martin in Martínkovice
- Church of St. Anne in Vižňov
- Church of St. Jakub Větší in Ruprechtice
- Church of St. Michal in Vernéřovice

- Church of All Saints in Heřmánkovice
- Church of St. Prokop in Bezděkov
- Church of St. Barbora in Otovice
- Church of St. Margaret in Šonov
- Church of St. Mary Magdalene in Božanov

The unique characteristics of these churches are that all of them were built in a quick time, most of them in 2-3 years. 8 out of 9 churches were designed by Kryštof Dientzenhofer and Kilián Ignác Dientzenhofer, father-son pair of architects.

The photographic details of these churches are documented in Appendix A.

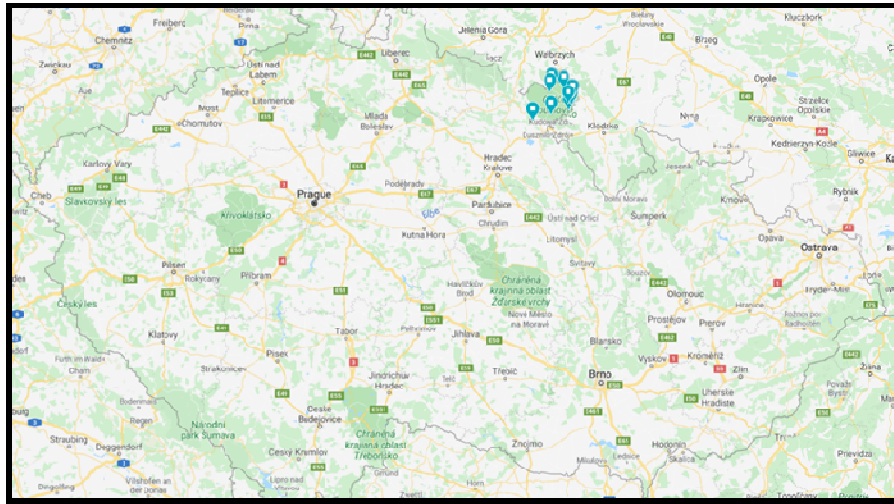





Figure 2.2 – Locations of Broumov churches marked on google maps(5)





This page is left blank on purpose.

### 3. STATE OF THE ART REVIEW

#### 3.1 Material – Sandstone

The table no 3.1 below shows the readily available types of sandstones in the region of Královéhradecký (6). There are a total of 8 quarries in the region. All testing procedure to calculate mechanical characteristics were done in accordance with EN-1926 (7) and EN12372 (8)

Stone	Appearance	Mechanical Characteristics	Example
Božanov Sandstone	Particle Size – Medium to coarse-grained Color – Light cream Presence of pigments – Possible Type of Pigment –ochre or red ferrous	Compressive strength = 68.9 MPa Flexural Strength = 5.2 MPa	 <p>Figure 3.1 – Božanov Sandstone</p>
Dubenec Sandstone	Particle Size -Fine-grained Color - light/ cream white Presence of pigments – Possible Pigment color –yellow up to red ferrous	Compressive strength = 46.5 MPa Flexural Strength = 4.9MPa	 <p>Figure 3.2 – Dubenec Sandstone</p>
Havlovice Sandstone	Particle Size -Fine-grained Type- Granular Color - ranges from typical light, cream to shades of dark orange, ochre or red Presence of pigments - Possible	Compressive strength = 131.2 MPa Flexural Strength = 8.3MPa	<p>Figure 3.3 – Havlovice Sandstone</p> 

<p>Bělohrad sandstone</p>	<p>Particle Size -Fine-grained Type- Marbled Color – reddish brown Presence of pigments - Possible</p>	<p>Compressive strength = 52.7 MPa Flexural Strength = 2.4MPa</p>	 <p>Figure 3.4 – Havlovice Sandstone</p>
<p>Kocbeře sandstone</p>	<p>Particle Size -Fine up to medium-grained Type- quartzose Color – light ivory color Presence of pigments – Possible ferrous</p>	<p>Compressive strength = 63.1 MPa Flexural Strength = 6.4MPa Young's modulus = 17.4 GPa(9)</p>	 <p>Figure 3.5 – Kocbeře Sandstone</p>
<p>Libná sandstone</p>	<p>Particle Size -Fine up to medium-grained Color – yellow to ochre Presence of fossils – Rarely Possible</p>	<p>Compressive strength = 74.3 MPa Flexural Strength = 5.9MPa Young's modulus = 22.5 GPa(9)</p>	 <p>Figure 3.6 – Kocbeře Sandstone</p>
<p>Hořice sandstone</p>	<p>Particle Size -Fine-grained Type- quartzose Color – light ochre base with ferrous coloring Presence of pigments – Possible Pigment color–yellowish-red ferrous</p>	<p>Compressive strength = 31.8 MPa Flexural Strength = 3.3MPa</p>	<p>Figure 3.7 – Hořice Sandstone</p> 



Trutnov sandstone	Particle Size – Coarse-grained  Color – shades of red	Compressive strength = 98.9 MPa  Flexural Strength = 6.7MPa	
			Figure 3.8 – Trutnov Sandstone
Záměl sandstone	Particle Size -Fine to medium-grained  Type- gloconite  Color – light color  Presence of pigments – Possible  Type of Pigment – various shades of grey ferrous pigments	Compressive strength = 60.1 MPa  Flexural Strength = 6.2MPa  Young's modulus = 22.5 GPa(9)	
			Figure 3.9 – Záměl Sandstone

Table 3.1 – Characteristics of locally found sandstone in the region of Královéhradecký.

### 3.1.1 Applicability of review

The walls of Broumov churches are stone masonry walls. During the review of existing literature and one visit to the Broumov region on June 11, 2020, it was confirmed that the majority portion of all wall assemblies was made from various types of sandstones with random typology. (grey, green, yellow and red color).

## 3.2 Masonry modeling strategies using finite element method

Numerical modeling of stone masonry walls can be approached in two different ways: Micro-modelling and macro-modeling(10). Both methods have their applications.

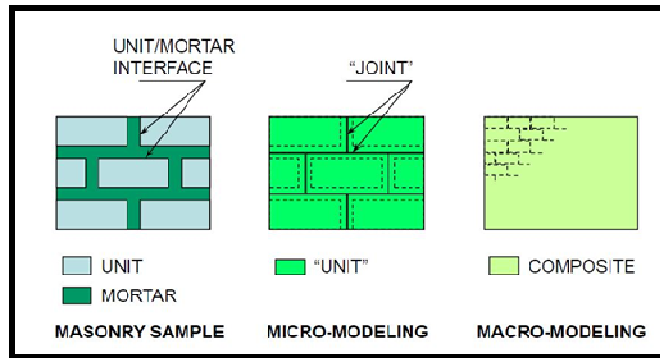


Figure 3.10 – Masonry assembly and Modelling types (11)

### 3.2.1 Detailed Micro-modeling

Micro-modelling allows users to accurately represent interface stresses with interface constitutive model. Masonry units are typically modeled as elastic-continuum elements and line elements with inelastic interface elements(10). The most accurate micromodel considers all failure mechanisms of masonry; Cracking of masonry joints, sliding failure, cracking, and crushing of masonry unit (11).

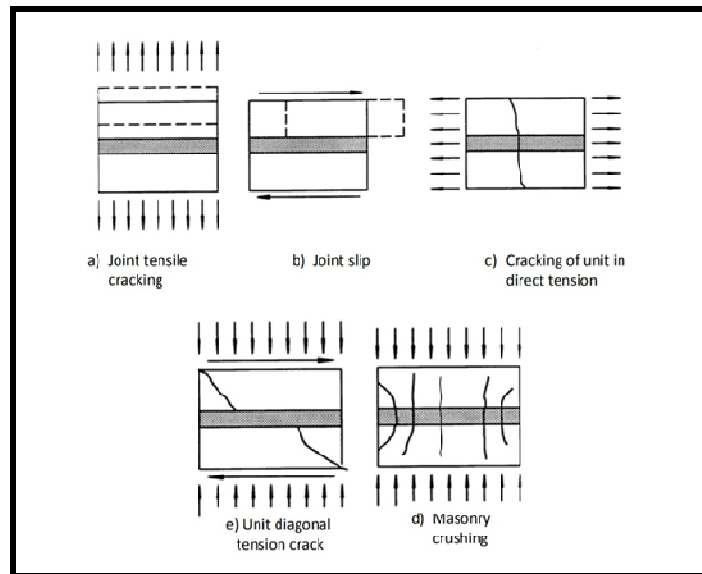


Figure 3.11 – Micromodel possible failure mechanisms (12)

### 3.2.2 Macro-modeling

Macro-modelling allows users to apply homogenized mechanical properties to masonry material with a constitutive material model. Typically, stone masonry walls are modeled as a one-element without



considering bricks/stones and mortar differently. Material is assigned to a homogeneous anisotropic continuum element. (10)

### 3.2.3 Homogenization techniques

Studies done during micro-modeling help more accurately understand the local behavior of masonry and help calculate realistic homogenized material properties to the large-scaled macro model. There are multiple approaches to homogenization: Micromechanical Approach, stress field expansion approach, etc.(10)

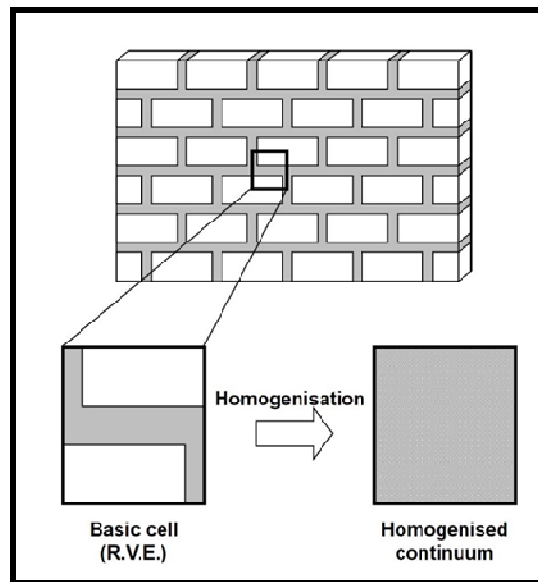


Figure 3.11 – Micro to macro-level through homogenization

### 3.2.4 Applicability of review

Broumov churches were constructed in the 1700s. Due to lack of maintenance and periodic monitoring, portions of wall finishes and paint have been spalled off/separated due to weathering and decay cycles, and wall bricklayer patterns and types of stones used for wall assembly are exposed.

2-D Micro-modelling approach (Detailed) is used in this thesis to numerically predict capacities of walls loaded under compression, in tension, and in-plane shear to plot stress-strain curves and evaluate crack patterns and deformation to help identify the mechanical properties of wall segments of broumov churches. It is understood that the results from this work with homogenization techniques will help evaluate and assign properties to full-scale 3D models of broumov churches.

### 3.3 Material Constitutive Model

Every material dissipates energy in a different way when external forces are applied to it. The amount of energy dissipation also depends on the direction of the forces. The constitutive models are the response of a material to mechanical and thermal loading. The models are generally constitutive equations of stress-strain relationships (13) and consider elastic, plastic, and fracturing components.

#### 3.3.1 Applicability of review

Non-linear finite element simulation program, Atena Engineering 2D, Version 5.7.0 was used for numerical calculations in this thesis. Atena program allows any material to assign a constitutive material model of the following types. (14)

Material Type	Description
Plane Stress Elastic Isotropic	Linear elastic material for 2D-plane stress state.
Plane Strain Elastic Isotropic	Linear elastic material for 2D-plane strain.
Axi Sym Elastic Isotropic	Lin. elastic for axially symmetrical stress state.
1D Elastic Isotropic	Linear elastic material for 1D reinforcement.
3D Cementitious	Fracture-plastic, linear compression.
3D Non-Linear Cementitious	Fracture-plastic, non-linear compression.
3D Non-Linear Cementitious 2	Same as above but fully incremental both in tension and compression. Recommended model for 2D and 3D concrete.
3D Variable Non-Linear Cem	Same as above but certain material parameters can vary during analysis.
3D Non-Linear Cem. User	Same as 3D Nonlinear Cem. 2, but the user can specify stress-strain relationships in tension, compression, shear and tension-compression interaction
Sbeta Material	SBETA material model, orthotropic smeared crack model. Suitable for plane stress 2D analysis.
Microplane4 Material	Bazant Micro-plane M4 Concrete
3D Bilinear Steel Von Mises	Von Mises plasticity.
2D Interface	Interface, cohesive, dry friction, gap.
Reinforcement	1D non-linear, bi-linear, multi-linear.
Cycling Reinforcement	1D Cyclic, Pinto-Menegoto.
Smeared Reinforcement	1D non-linear, bi-linear, multi-linear.
Spring	1D linear, multi-linear,
Bond for Reinforcement	Bond-slip relation.
3D Drucker-Prager	Plasticity Drucker-Prager plasticity.

Material With Random Fields	Material for random field generation. Can be used together with any of the above materials and in connection with the SARA program to generate material with the spatial distribution of selected material parameters.
-----------------------------	--

Table 3.2 – Atena user's manual Part 2-1 Table 4-1 (14)

In Atena program, every material model has a default set of parameters that can be revised per applicable findings to improve the response of the model. The typical material type has its inbuilt constitutive law and failure criteria/law based on CEB-FIP Model code 90.

During the numerical calculations of uniaxial compression, tension, and shear tests, material model 3D Non-linear Cementitious 2 model was used to simulate the behavior of 2D models. 3D Non-linear Cementitious 2 model is a fracture plastic model that includes a constitutive model for tensile fracturing (Rankine Fracture model) and compressive plastic behavior. 3D Non-linear Cementitious 2 model also considers the hardening regime before reaching compressive strength(15). Atena uses updated langrange formulation to compute continuum governing equations to solve the nonlinear problem.

### 3.4 Discretization using finite element method

The finite Element Method is a numerical approach to solve partial differential equations. The method divides the body into finite elements (quadrilaterals or triangular elements) with the technique of mesh discretization and obtains an approximate solution. The finite elements can be 2D/3D isoparametric elements, beam elements, plate elements, special truss and cable elements, springs, and interfaces.

#### 3.4.1 Applicability of review

There are multiple approaches in solid mechanics which can be used for Numerical estimations of boundary value problem. For example Finite element method (FEM), limit analysis, and discrete element method. This thesis uses FEM approach for numerical analysis.

During the numerical calculations of uniaxial compression, tension and shear tests, Plane stress 2D isoparametric 8 node element (CCIsoQuad) of size 1 cm was used. Mesh generation was achieved with a combination of both quadrilateral and triangular finite elements. Interface elements were introduced to model contact between masonry and mortar

This page is left blank on purpose.

## 4. EXPERIMENTAL TEST PROCEDURES

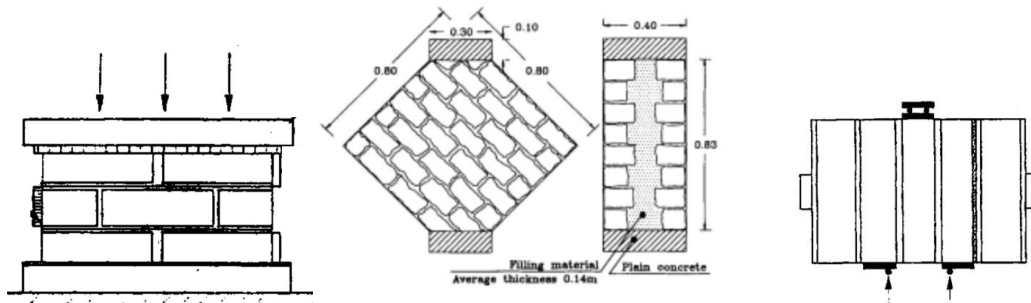


Figure 4.1 – Experimental test setups - Compression test (left), diagonal compression test (middle), in-plane shear test (right)

### 4.1 Determination of Compressive strength in accordance with BS EN 1052-1:1999

BS EN 1052-1:1999 explains the experimental test procedure to determine the compressive strength of masonry perpendicular to the bed joint. 1m long x 1m tall x 0.5m thick specimen fits the criteria for specimen configuration.(16) After the curing of the specimen, the standard requires to test the strength of masonry and strength of mortar on the same day.

Test procedure:

The specimen is placed centrally in the testing machine. To ensure the equal load distribution of forces, steel plates of equal or longer length than the specimen are attached at the top and bottom of the specimen. Once the testing setup is complete, the load is then applied uniformly from the top and bottom of the specimen to obtain load-displacement/machine extension readings.

Standard suggests reaching failure in between 15-30 min mark from the application of load. Standard allows applying a method of either constant incremental load or constant rate of displacement.

Compressive strength of the specimen is calculated as:

$$f_i = F_{i,max} / A_i \quad (\text{eq.1})$$

$F_{i,max}$  = Maximum load reached on masonry specimen (N)

$A_i$  = loaded cross-section of an individual masonry specimen (mm<sup>2</sup>)

$f_i$  = compressive strength of individual masonry specimen (N/mm<sup>2</sup>)

Annex A of the standard gives equation to calculate the compressive strength of masonry from compressive strengths of masonry units and compressive strengths of mortar as equation 2.

$$f_{id} = f_i \times (f_{bd}/f_b)^{0.65} \times (f_{md}/f_m)^{0.25} \quad (\text{eq. 2})$$

$f_{id}$  = adjusted individual masonry compressive strength (N/mm<sup>2</sup>)

$f_i$  = compressive strength of individual masonry specimen (N/mm<sup>2</sup>)

$f_{bd}$  = specific mean compressive strength of masonry unit (N/mm<sup>2</sup>)

$f_b$  = mean compressive strength of the masonry unit at the time of masonry test (N/mm<sup>2</sup>)

$f_{md}$  = specific mean compressive strength of mortar (N/mm<sup>2</sup>)

$f_m$  = mean compressive strength of mortar at the time of masonry test (N/mm<sup>2</sup>)

## 4.2 Diagonal Compression Test in accordance with ASTM E519-02

ASTM E519-02 (17) explains the test procedure and experimental method to calculate the shear strength (diagonal tension) of 1.2m x 1.2m (4 ft x 4 ft) masonry assembly. When masonry wall specimen is loaded in compression at one diagonal of the specimen, diagonal tension failure can be achieved with cracks propagating along the direction parallel to the direction of the load.

Test procedure:

2 loading shoes are placed at the center of the testing specimens as shown in Figure 4.1. Compressometers and extensometers are used to measure the shortening of vertical diagonal and elongation of horizontal diagonal. Once the testing setup is complete, the load is then applied in increments to obtain load- displacement and stress-strain curve.

Standard recommends a minimum of 10 load steps for a smooth curve and minimum 3 test samples for better accuracy of the results. Ultimate load up to failure can be observed experimentally.

Tensile strength of specimen is calculated as:

$$S_s = 0.707 \times P / A_n \quad (\text{eq. 3})$$

$$A_n = \frac{1}{2} \times (w + h) \times t \times n \quad (\text{eq. 4})$$

$S_s$  = shear stress on net area (MPa)

$P$  = Applied load (N)

$A_n$  = net area of the specimen ( $\text{mm}^2$ )

$w$  = width of specimen (mm)

$h$  = height of specimen (mm)

$t$  = total thickness of specimen (mm)

$n$  = percentage of the gross area of the unit that is solid, expressed as a decimal

Tensile strength  $f_t = 0.707 \times P_{\max} / A_n$  (eq. 5)

$P_{\max}$  = Maximum applied load (N)

### **4.3 Measurement of in-plane shear strength of masonry mortar joint in accordance with ASTM C1531-02**

Push test in accordance with ASTM C1531-02 (18) directly calculates shear resistance of the mortar joint in masonry. Results from push tests work well for relatively strong units and weak mortar. There are three minor destructive test methods, test methods A, B and C.

Standard recommends a minimum of 8 test locations per building for better accuracy of the results.

Test Procedure: There are possible 3 ways to conduct this test.

Test A requires the use of 2 flat jacks, above and below test unit. Flat jack controls vertical compressive stresses at the location of the shear test. The hydraulic ram is used to apply load in the horizontal direction. The ratio between the joint shear strength index and compressive stresses calculates the coefficient of friction of the unit-mortar interface.

Test B is tested by lateral displacement of single stone relative to adjacent stone in the same wythe. The head joint next to the loaded end is cleared and the stone adjacent to the test stone is removed for steel loading blocks and hydraulic ram. Steel blocks are used to distribute the load to the stone without touching the mortar joint. The load is then applied in a horizontal direction until crack or slip occurs. In-plane shear strength of mortar is calculated by the ratio between load at first crack or movement and a nominal gross area of the sum of 2-bed joints. The coefficient of friction is assumed based on previous research/ method A or lab results.

Test C requires the use of a special flat jack for the application of a horizontal load on the test unit. Only head joints at each side of the test sample unit are required to be cleaned and adjacent masonry units are kept as is due to the use of special flat jack for application of horizontal load without hydraulic ram. Flat jack is inserted into one end of the test unit head joint. A horizontal force is calculated by recorded hydraulic pressure in the flat jack and in-plane shear strength and joint shear strength index are calculated as test B.



## 5. NUMERICAL ANALYSIS

### 5.1 Wall Topology and Model Geometry

Broumov churches were constructed in the 17<sup>th</sup> and 18<sup>th</sup> centuries with a typical wall system consisting of irregular stone rubble masonry units and natural hydraulic lime mortar. From observations and past work from Broumov churches, the stone topologies of Grey sandstone, yellow sandstone, red sandstone, green sandstone, bricks, and ignimbrite stones were observed.

Four different masonry wall arrangements from different Broumov churches were chosen to analyze the behavior in compression, tension, and shear with analysis program Atena 2D. The geometry was directly modeled in Atena 2D. All cross-sections were modeled as 1m x 1m in cross-section. 0.5 m thickness was assigned to the 2D modeled stones and mortar. Gap interface was assigned between the stone and mortar at a bed and head joints. The interface material model with tensile softening is based on Mohr-Coulomb criteria which consider interfacial failures and slips.

Since the mortar is the weakest link in masonry; to avoid early failure, the width of the head and bed joints was kept between 0.01m to 0.02m

2D WALL	WALL SIZE	TOTAL NUMBER OF ELEMENTS USED		
		JOINTS	LINES	MACROELEMENTS
Wall Assembly 1	1m x 1m	438	533	94
Wall Assembly 2	1m x 1m	455	594	140
Wall Assembly 3	1m x 1m	427	573	147
Wall Assembly 4	1m x 1m	544	745	202

Table 5.1– Wall assembly model information

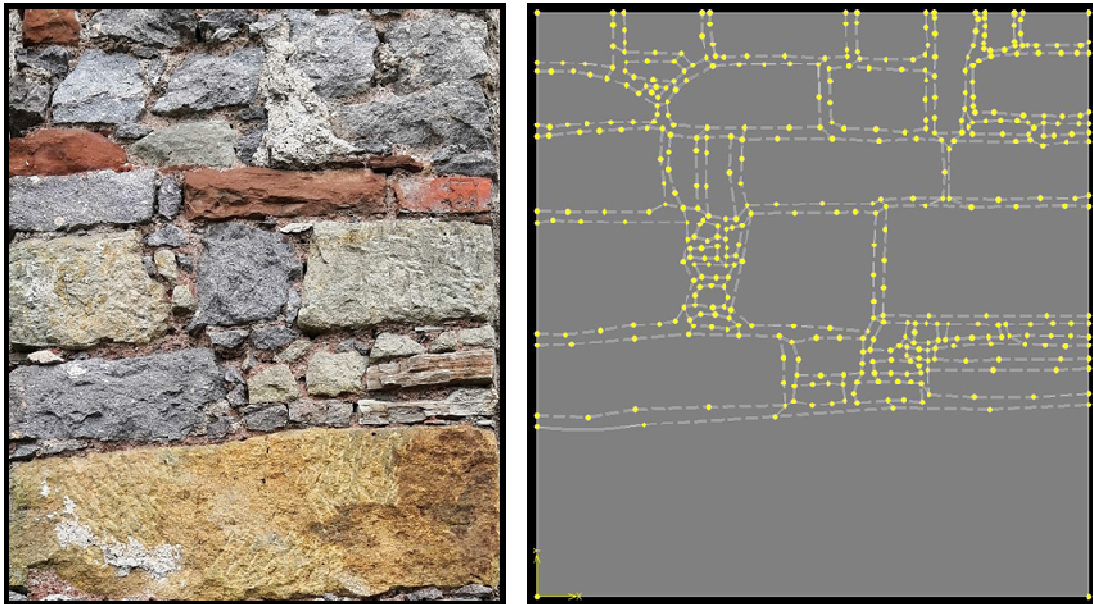


Figure 5.1- As-built wall assembly 1 (left), Atena 2D model configuration (right)



Figure 5.2- As-built wall assembly 2 (left), Atena 2D model configuration (right)



Figure 5.3- As-built wall assembly 3 (left), Atena 2D model configuration (right)

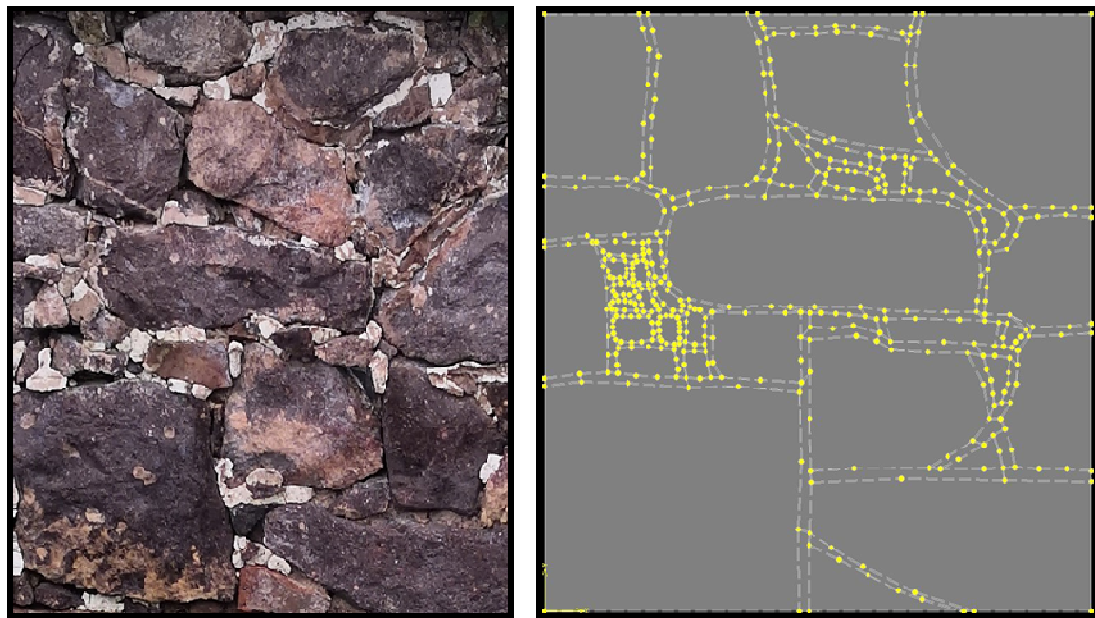


Figure 5.4- As-built wall assembly 4 (left), Atena 2D model configuration (right)

## 5.2 Masonry Arrangement and MQI

Due to 'Covid-19' lockdown regulations, frequent visits to the Broumov region were not feasible and any minor or nondestructive tests or laboratory experiments were not conducted during this study. To estimate the quality of masonry, Masonry Quality Index (MQI) method was used for preliminary calculations. With the technique of masonry quality index, it is possible to assess historical masonry by evaluating presence, partial presence, or the absence of the following parameters. (19)

- SM: Stone/brick mechanical properties and conservation state
- SD: Unit dimension properties
- SS: Unit shape
- WC: Wall leaf connection
- HJ: Horizontal bed joint characterization
- VJ: Vertical bed joint characterization
- MM: Mortar mechanical properties

Based on the parameters, MQI is evaluated as,

$$MQI = SM * (SD + SS + WC + HJ + VJ + MM). \quad (19)$$

Each parameter can have three possible outcomes as fulfilled (F), partially fulfilled (PF), and not fulfilled (NF). For different loading types, based on final MQI values obtained from engineering judgments, masonry can be classified in category A, category B, and category C per the table below

Loading type	Masonry Category		
	Category A	Category B	Category C
Vertical Loads	$5 \leq MQI \leq 10$	$2.5 \leq MQI \leq 5$	$0 \leq MQI \leq 2.5$
Out of Plane Loads	$7 \leq MQI \leq 10$	$4 \leq MQI \leq 7$	$0 \leq MQI \leq 4$
In-Plane Loads	$5 \leq MQI \leq 10$	$3 \leq MQI \leq 5$	$0 \leq MQI \leq 3$

Table 5.2– Classification of masonry according to the method of MQI (19)

To calculate the MQI for classical bricklayer's masonry assembly, considered loading conditions were vertical loading and in-plane loads since out of plane behavior of the masonry is not part of this study. Wall leaf connections were not confirmed and will be considered good with the presence of through-stones between the wythe since no horizontal cracks were observed during the past and present investigation.

### 5.2.1 Vertical Loading

Wall Assembly 1			Wall Assembly 2		
SM	F	1	SM	PF	0.7
SD	F	1	SD	PF	0.5
SS	PF	1.5	SS	PF	1.5
WC	F	1	WC	F	1
HJ	PF	1	HJ	PF	1
VJ	PF	0.5	VJ	PF	0.5
MM	PF	0.5	MM	F	0.5

Table 5.3– Calculation of MQI Parameters under vertical loading – Wall assembly 1 (Left), Wall assembly 2 (Right)

Wall Assembly 3			Wall Assembly 4		
SM	PF	0.7	SM	PF	0.7
SD	PF	0.5	SD	PF	0.5
SS	PF	1.5	SS	PF	1.5
WC	F	1	WC	F	1
HJ	PF	1	HJ	NF	0
VJ	PF	0.5	VJ	NF	0
MM	NF	0	MM	NF	0

Table 5.4– Calculation of MQI Parameters under vertical loading – Wall assembly 3 (Left), Wall assembly 4 (Right)

VERTICAL LOADING	MQI	MASONRY CATEGORY	QUALITY OF MASONRY
Wall Assembly 1	5.5	Category A	Good behavior
Wall Assembly 2	3.5	Category B	Average quality behavior
Wall Assembly 3	3.15	Category B	Average quality behavior
Wall Assembly 4	2.1	Category C	Inadequate behavior

Table 5.5– Calculation of MQI and quality of the masonry

### 5.2.2 In-plane Loading

Wall Assembly 1		
SM	F	1
SD	F	1
SS	PF	1
WC	F	2
HJ	PF	0.5
VJ	PF	1
MM	PF	1

Wall Assembly 2		
SM	PF	0.7
SD	PF	0.5
SS	PF	1
WC	F	2
HJ	PF	0.5
VJ	PF	1
MM	F	2

Table 5.6– Calculation of MQI Parameters under lateral loading – Wall assembly 1 (Left), Wall assembly 2 (Right)

Wall Assembly 3		
SM	PF	0.7
SD	PF	0.5
SS	PF	1
WC	F	2
HJ	PF	0.5
VJ	PF	1
MM	NF	0

Wall Assembly 4		
SM	PF	0.7
SD	PF	0.5
SS	PF	1
WC	F	2
HJ	NF	0
VJ	NF	0
MM	NF	0

Table 5.7– Calculation of MQI Parameters under vertical loading – Wall assembly 3 (Left), Wall assembly 4 (Right)

IN-PLANE LOADING	MQI	MASONRY CATEGORY	QUALITY OF MASONRY
Wall Assembly 1	6.5	Category A	Good behavior
Wall Assembly 2	4.9	Category B	Average quality behavior
Wall Assembly 3	3.5	Category B	Average quality behavior
Wall Assembly 4	2.45	Category C	Inadequate behavior

Table 5.8– Calculation of MQI and quality of the masonry

### 5.2.3 Evaluation of strength parameters using MQI

From MQI, through correlation, it is possible to obtain an estimate of some mechanical parameters such as - compressive strength, shear strength, and young's modulus of elasticity.

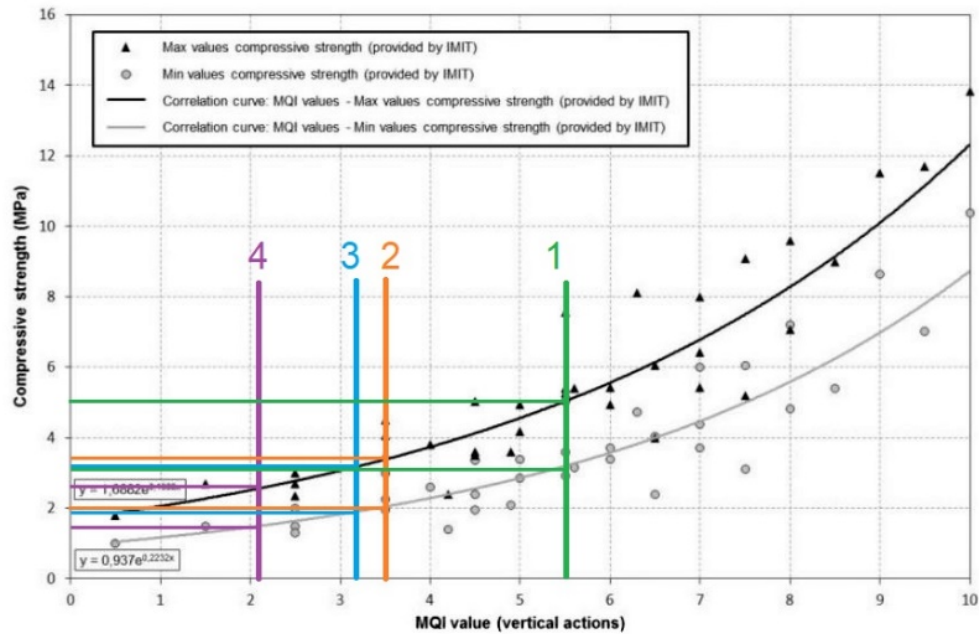


Figure 5.5– Correlation curves: MQI values vs compressive strength

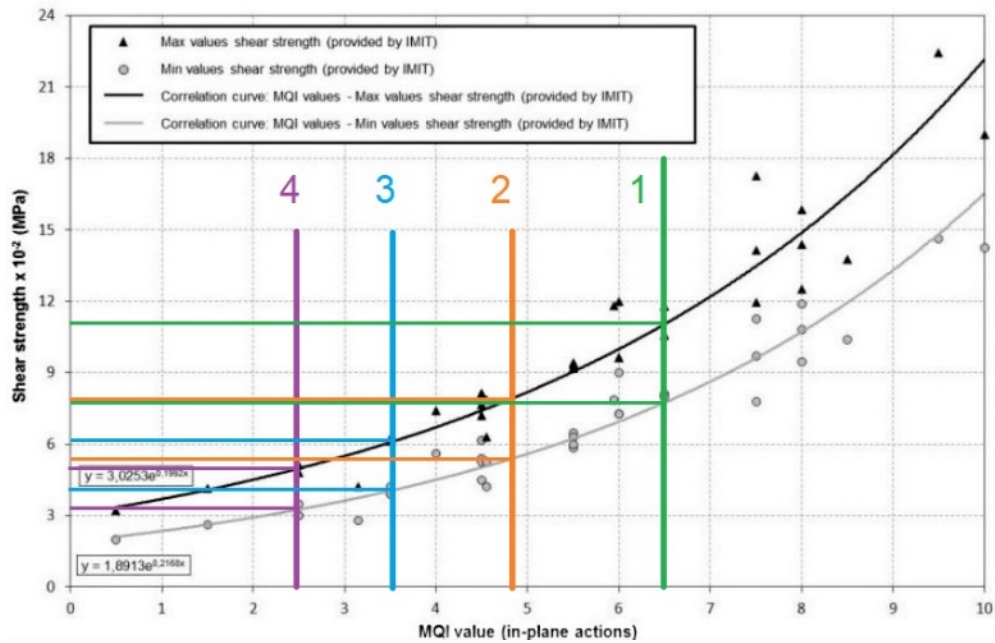


Figure 5.6– Correlation curves: MQI values vs shear strength

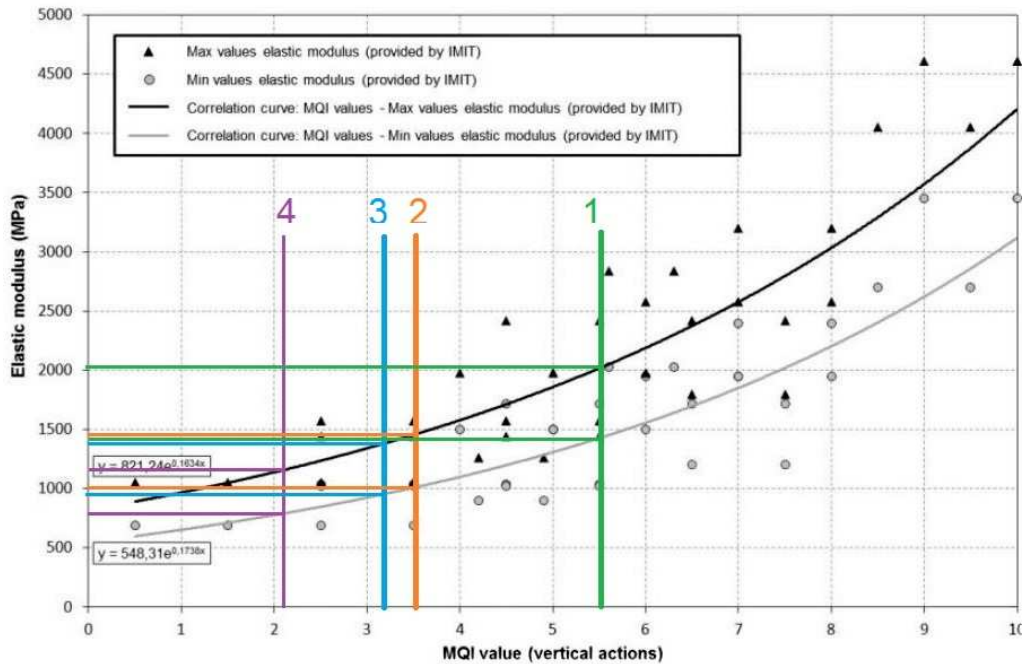


Figure 5.7– Correlation curves: MQI values vs Young’s modulus of elasticity

	MQI	COMPRESSIVE STRENGTH $f_m$ [MPa]	SHEAR STRENGTH $\tau_0$ [MPa]	YOUNG’S MODULUS $E$ [MPa]
Wall Assembly 1	5.5	3.1 - 5.0	0.077 - 0.110	1450 - 2010
Wall Assembly 2	3.5	2.0 - 3.3	0.052 - 0.080	1000 - 1470
Wall Assembly 3	3.15	1.9 - 3.1	0.038 - 0.061	950 - 1420
Wall Assembly 4	2.1	1.7 - 2.6	0.031 - 0.050	800 - 1200

Table 5.9– Estimations of strength parameters of masonry wall assemblies using MQI method

### 5.3 Material Properties and Constitutive material model

Since the effect of multi leaves in the third direction were not modeled for 2D analysis, reduced material parameter computed in past studies were applied during the non-linear analysis. Material and geometric non-linearity were considered in the Atena 2D calculations. Atena program can present the real behavior by considering the additional internal forces developed by cracking, and crushing under high confinement and redistributing them within the finite element model.



Atena program mainly focuses on the reinforced concrete structure so the material model needs to behave like stone masonry elements. "3D Non-Linear Cementitious 2" material model was used. It is a fracture-plastic constitutive model with the orthotropic smeared crack formulation and crack band model. (15)

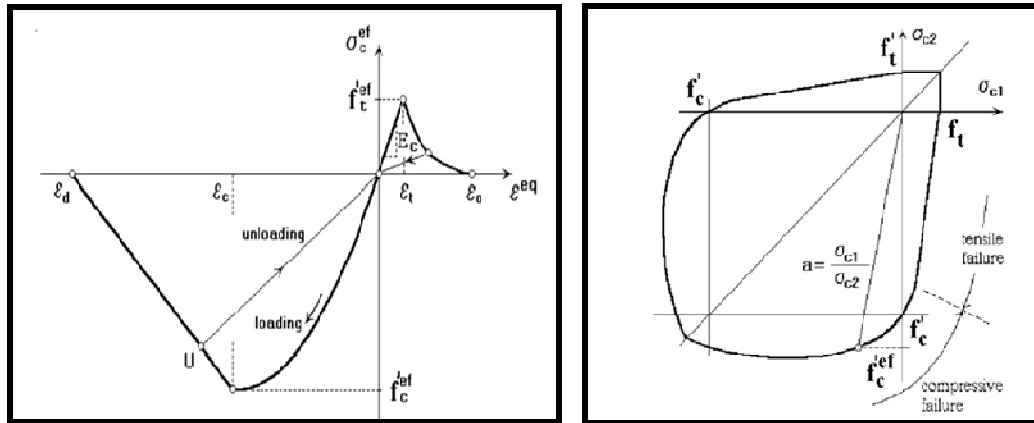


Figure 5.9– Uni-axial stress-strain law (left), Biaxial failure function (right) (15)

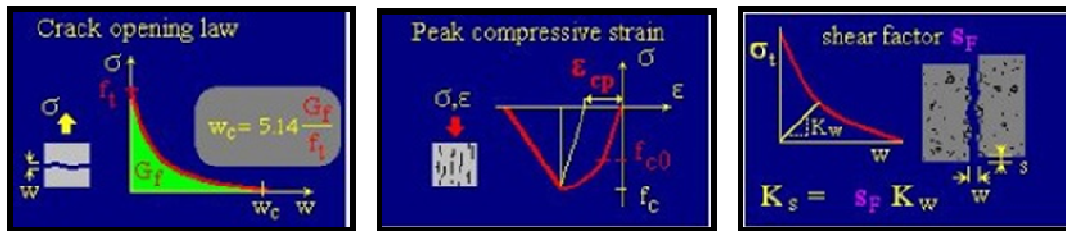


Figure 5.10– Exponential crack opening law in tension. Stress- crack width diagram (left), Compressive stress-strain diagram (middle) Exponential crack opening law in shear. Stress- crack width diagram (right)

Material	Young's Modulus E [GPa]	Poisson's ratio $\nu$ [unitless]	Tensile strength $f_t$ [MPa]	Compressive strength $f_c$ [MPa]	Tensile Fracture Energy $G_f$ [N/m]	Peak compressive strain $\epsilon_{CP}$ [unitless]	Unit weight $\rho$ [kN/m <sup>3</sup> ]
Red Sandstone	20	0.2	1.5	30	43.5	0.0015	21
Grey Sandstone	13	0.2	2	20	58	0.0015	21
Green Sandstone	8	0.2	1.0	12	34.8	0.0015	21

<b>Yellow Sandstone</b>	7.51	0.2	2.9	29	35	0.0015	21
<b>Ignimbrite</b>	9.49	0.2	4.2	42	60	0.0015	21
<b>Rubble</b>	0.7	0.2	0.1	2	10	0.0029	20
<b>Bricks</b>	4.2	0.2	1.85	18.5	130	0.0036	18.7
<b>Lime Mortar</b>	0.126	0.17	0.1	1.5	10	0.0012	20
<b>Steel plate</b>	200	0.3	-	-	-	-	-

Table 5.10– Summary of material properties obtained from past studies (20, 21)

## 5.4 Numerical Model

Numerical models were prepared using Atena 2-D. Finite element mesh was generated with Plane stress 2D Isoparametric 8 node low order element (CCIsoQuad) with a combination of quadrilaterals and triangles elements of size 0.01m. Material and geometric nonlinearity was assigned for post-peak behavior. For each test load conditions, supports and solution parameters are specified below.

### 5.4.1 Compression Test

Load cases:

Supports	The bottom line of wall specimen is fixed in the vertical direction
Supports	The bottom left corner is fixed in the horizontal direction
Load	Self-weight of the wall specimen
Load	The top line of wall specimen is loaded by a prescribed uniform displacement of 0.5 mm in vertical negative Y- direction for compression.

Solution Parameters:

Solution method	Newton- Raphson
Stiffness/update	Tangent/each iteration
Number of iterations	50
Error tolerance	0.01
Line search	On, with iterations

Finite element mesh:

Finite element type	Mixed, CCIsoQuad
Finite element size	0.01 m
Element shape smoothing	On
Geometric nonlinearity	On

Optimization	Sloan
--------------	-------

#### 5.4.2 Tension Test

Load cases:

Supports	The bottom line of wall specimen is fixed in the vertical and horizontal direction
Load	Self-weight of the wall specimen
Load	The top line of wall specimen is loaded by uniform linear force $1 \times 10^{-3}$ MN/m in vertical positive Y- direction for tension.

Solution Parameters:

Solution method	Newton- Raphson
Stiffness/update	Tangent/each iteration
Number of iterations	50
Error tolerance	0.01
Line search	On, with iterations

Finite element mesh:

Finite element type	Mixed, CCIsoQuad
Finite element size	0.01 m
Element shape smoothing	On
Geometric nonlinearity	On
Optimization	Sloan

#### 5.4.3 In-plane Shear Test

Load cases:

Supports	The bottom line of wall specimen is fixed in the vertical direction
Supports	The right line of wall specimen is fixed in the horizontal direction
Load	Self-weight of the wall specimen
Load	The left line of the wall specimen is loaded by uniform linear force $1 \times 10^{-3}$ MN/m in horizontal negative X- direction for in-plane shear.

Solution Parameters:

Solution method	Newton- Raphson
Stiffness/update	Tangent/each iteration
Number of iterations	50
Error tolerance	0.01

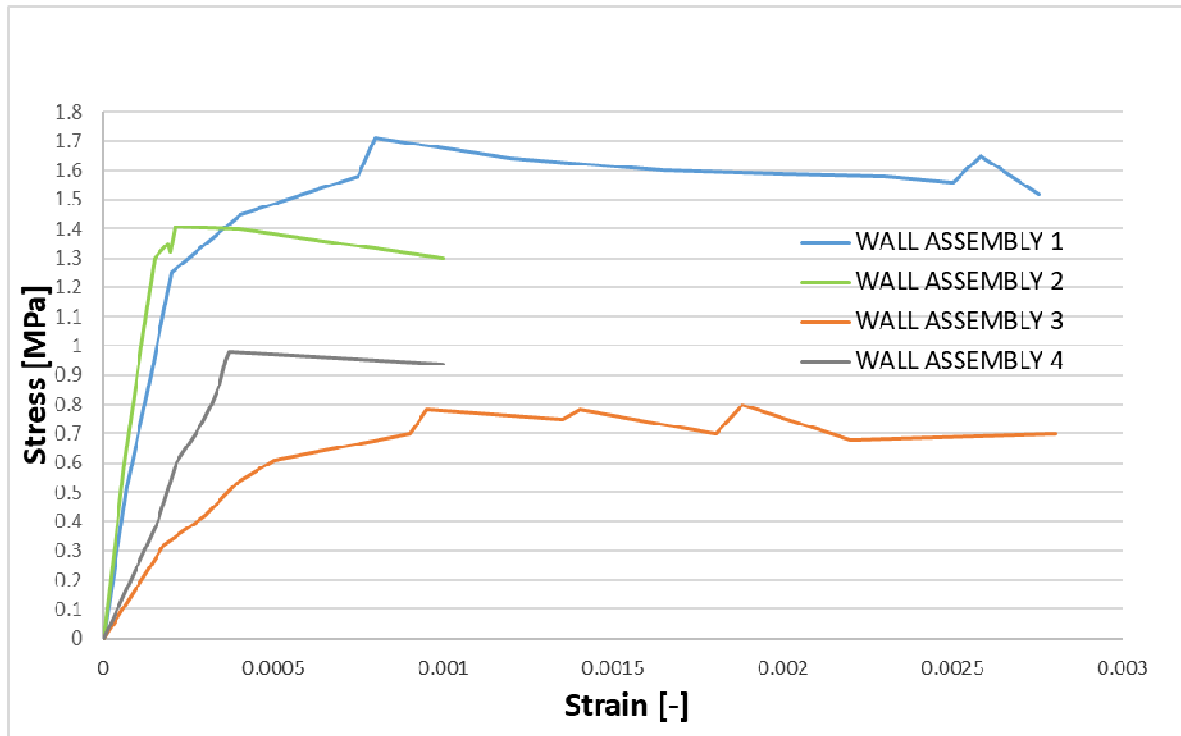
Line search	On, with iterations
-------------	---------------------

Finite element mesh:

Finite element type	Mixed, CCIsoQuad
Finite element size	0.01 m
Element shape smoothing	On
Geometric nonlinearity	On
Optimization	Sloan

## 6. RESULTS

### 6.1 Compression Test



Graph 6.1– Comparison between Compressive Stress vs Strain curves

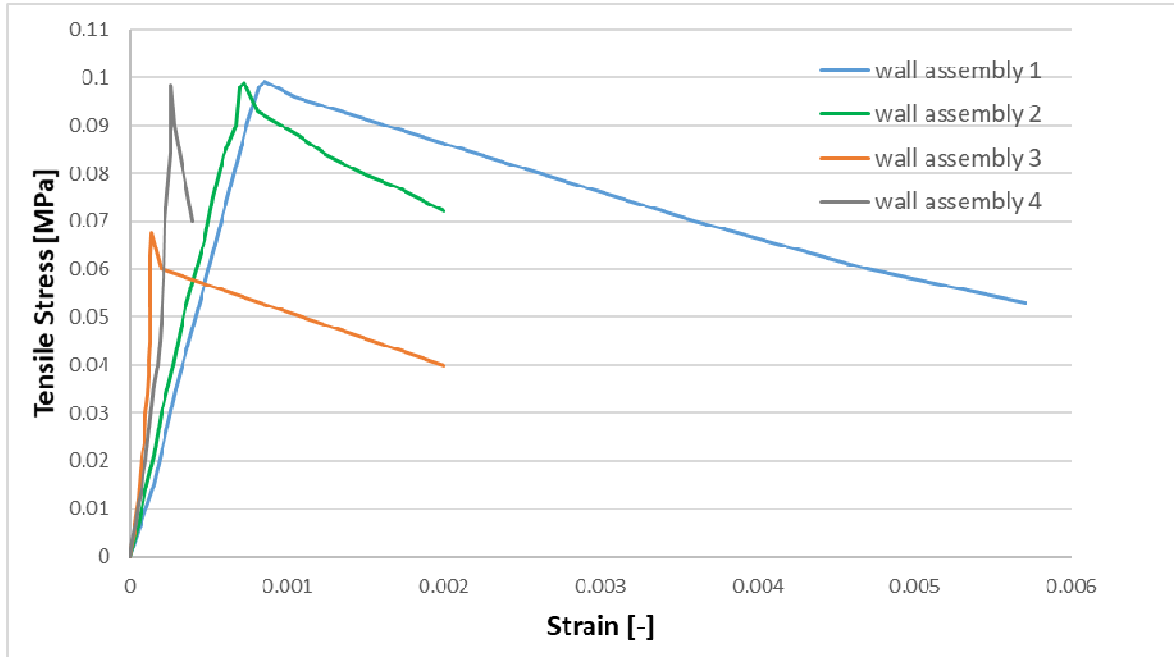
Wall assembly	Peak compressive stress (MPa)	Compressive strain at peak stress
1	1.71	0.0008
2	1.40	0.0004
3	0.79	0.0009
4	0.98	0.0004

Table 6.1 – Comparison between Compressive Stress and Strain values of wall assemblies

Standard deviation	0.414	0.00026
Average	1.22	0.000625
COV	33.96%	42.08%

Table 6.2 – Standard deviation, average, and Coefficient of variation between wall assemblies 1 through 4

## 6.2 Tension Test



Graph 6.2– Comparison between Tensile Stress vs Strain curves

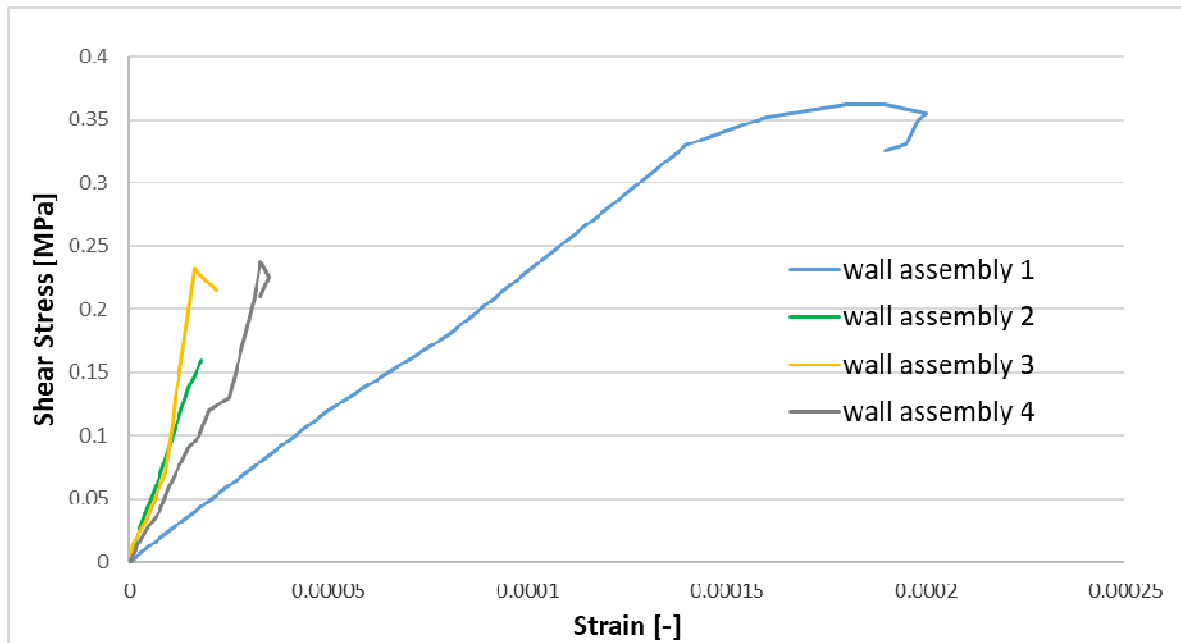
Wall assembly	Peak tensile stress (MPa)	Strain at peak tensile stress
1	0.099	0.00086
2	0.099	0.00073
3	0.067	0.00013
4	0.098	0.00026

Table 6.3 – Comparison between Compressive Stress and Strain values of wall assemblies

Standard deviation	0.016	0.00035
Average	0.09075	0.000495
COV	17.45%	71.61%

Table 6.4 – Standard deviation, average, and Coefficient of variation between wall assemblies 1 through 4

### 6.3 Shear Test



Graph 6.3– Comparison between Shear Stress vs Strain curves

Wall assembly	Peak shear stress (MPa)	Strain at peak shear stress
1	0.362	0.00018
2	0.163	0.0000187
3	0.232	0.000017
4	0.238	0.000033

Table 6.5– Comparison between Compressive Stress and Strain values of wall assemblies

Standard deviation	0.083	0.00042
Average	0.248	0.000232
COV	33.29%	180.30%

Table 6.6 – Standard deviation, average, and Coefficient of variation between wall assemblies 1 through 4

Standard deviation	0.042	0.00001
Average	0.211	0.0000229
COV	19.75%	38.38%

Table 6.7 – Standard deviation, average, and Coefficient of variation between wall assemblies 2 through 4

This page is left blank on purpose.



## 7. DISCUSSION

### 7.1 Compression Test

- Wall assemblies 1-4 were analyzed to compare crack development in masonry mortar and principal plastic strain under uniaxial compression (-Y direction). The principal plastic strain is a component of strain corresponding to crack opening. See Appendix B.
- Compressive Stress vs strain plots were generated to compare and evaluate the bricklayer's pattern with identical properties of hydraulic lime mortar. As predicted, most cracks appeared in the mortar, and failure due to compressive crushing and tensile splitting was observed.
- From results, wall assembly 1 performed best in compression and allowed compressive stress of 1.71MPa which is consistent with MQI results. It is partly because there is only 1 stone in the bottom layer of wall assembly 1.
- According to MQI characterization, wall assembly 4 should have performed the worst out of the four assemblies tested. But due to modeling simplification and presence of relatively larger stones in wall assembly 4, wall assembly 3 performed the worst with Peak compressive stress of 0.79 MPa
- The small stones near to the left bottom side of wall assembly 2 and 3 were overstressed early and reached peak compressive stress relatively earlier with a lower strain value of 0.0004.
- Irregularity in topology created areas of high stress concentrations which ultimately reduced overall compressive strength of the wall.

### 7.2 Tension Test

- Wall assemblies 1-4 were analyzed to compare crack development in masonry mortar and principal plastic strain under uniaxial tension (+Y direction). See Appendix B.
- Tensile Stress vs strain plots were generated to compare and evaluate the bricklayer's pattern with identical properties of hydraulic lime mortar. As predicted, crack development was observed in mortar joints through the easiest path possible.
- The model resulted in the tensile strength of masonry close to mortar tensile strength.
- Wall assembly 1 performed best in uniaxial tension and allowed tensile stress of 0.099 MPa which is consistent with MQI results.
- Similar to uniaxial compression test wall assembly 3 performed the worst with Peak tensile stress of 0.067 at strain equal to 0.00013.

- Wall assembly 3 showed the brittle failure mechanism with other assemblies showed a quasi-brittle failure mechanism. This might be due to convergence issue with large crack widths
- Wall assemblies 1,2 and 4 showed similar peak tensile stress values close to 0.1MPa at different strain values ranging from 0.00026-0.00086.

### 7.3 Shear Test

- Wall assemblies 1-4 were analyzed with loads applied in in-plane shear (-X direction) to compare the formation and development of vertical crack. Max. principal stress and principal plastic strains were observed and documented in Appendix B.
- Shear Stress vs strain plots were generated to compare and evaluate the bricklayer's pattern. Crack development was observed in mortar head joints through the easiest path possible close to the location of applied loading. Failure can be assumed by the splitting of masonry.
- Wall assembly 1 performed best in the shear test due to the presence of 1 large stone in the bottom layer. Wall assembly 1 showed higher strength and stiffness than the rest of the wall assemblies with a max shear stress of 0.3MPa and associated strain of 0.00086.
- Wall assembly 2 performed the worst between the four with Peak shear stress of 0.163 at strain equal to 0.000019 due to the presence of smaller stones near the left side of the assembly.

### 7.4 Validation of Results

Wall Assembly	Compressive Strength $f_c$ [MPa]	Estimation of Compressive Strength by MQI method $f_m$ [MPa]	Tensile Strength $f_t$ [MPa]	Estimation of Tensile Strength as 10 percent of Compressive Strength $f_t$ [MPa]	Shear Strength $\tau_0$ [MPa]	Estimation of Shear Strength by MQI method $\tau_0$ [MPa]
1	1.71	3.1 - 5.0	0.099	0.31-0.5	0.362	0.077- 0.110
2	1.4	2.0 - 3.3	0.099	0.2-0.33	0.163	0.052 - 0.080
3	0.79	1.9 - 3.1	0.067	0.19-0.31	0.232	0.038 - 0.061
4	0.98	1.7 - 2.6	0.098	0.17-0.26	0.238	0.031 - 0.050

Table 7.1– Comparison between strength parameters of wall assemblies

Type of masonry	Characteristic Compressive Strength based on NTC 2018 and 2019 commentary $f_k$ [MPa]	Average Compressive strength obtained from numerical calculations $f_c$ [MPa]
Uncut stone masonry with leaves of irregular thickness	2.0 - 3.3	1.22

Table 7.2– Comparison between average compressive strength of wall assemblies and recommended values from NTC 2018 and 2019 commentary

Type of masonry	Characteristic Shear Strength based on NTC 2018 and 2019 commentary $\tau_0$ [MPa]	Average Shear Strength obtained from numerical calculations $\tau_0$ [MPa]
Uncut stone masonry with leaves of irregular thickness	0.035 – 0.051	0.24

Table 7.3– Comparison between average shear strength of wall assemblies and recommended values from NTC 2018 and 2019 commentary

This page is left blank on purpose.

## 8. CONCLUSION AND FUTURE RECOMMENDATIONS

In conclusion, masonry's strength parameters computed in this study using numerical calculations are tabulated below. Relatively lower strength in compression than expected and high strength in shear was observed in this study. Bricklayer's arrangement directly impacted the resistance to applied loading in tension shear and compression and strength parameters of the wall.

Wall Assembly	Compressive Strength $f_c$ [MPa]	Tensile Strength $f_t$ [MPa]	Shear Strength $\tau_0$ [MPa]
1	1.71	0.099	0.362
2	1.4	0.099	0.163
3	0.79	0.067	0.232
4	0.98	0.098	0.238

Table 8.1– Comparison between strength parameters of wall assemblies

Numerical results were validated by comparing the results with estimated values from the MQI method and suggested values of masonry properties in Italian NTC 2018 and 2019 commentary. MQI method would not be the most accurate method since the parameters are calculated by the engineer's judgment against numerical calculations using FE models.

The average compressive strength calculated by numerical calculation is 1.22 MPa. The walls are currently experiencing around compressive stresses of 0.5 MPa so it can be concluded that the walls are safe under gravity loading at a current stage.

During shear calculations in 2D, with dimensions of micromodel were working as plane strain case where an increase in stress doesn't cause an increase in strain and ultimately brittle failure. In reality, as walls are tall and slender, the behavior is more plane stress and shear strength values can be lower than predicted by the numerical micro-model.

Tensile strengths of masonry were found close to the tensile strengths of binding material in this case hydraulic lime mortar. This behavior is predictable and looked satisfactory.

Future recommendations:

Models can be further improved by improving the geometry of the model, especially by including arc elements in addition to line elements near the corner of the stone units since corners of weathered stone are more round than straight lines.

ASTM E519-02 recommends using a wall dimension of 1.2 m x1.2 m for tension test. It would be interesting to observe and to compare the results based on different sizes of wall specimens.

In-plane shear strength of wall specimen when loaded in other X-direction would provide different results due to randomness of topology and it would be nice to calculate results in other in-planer direction and compare the results.

With a gradual increase in the height to thickness slenderness ratio, it would be nice work to compare the results in shear test and plot graphs of reduction in shear strength as per increase in slenderness ratio.

Since Atena is mainly used for FE analysis of reinforced concrete structures, more specific constitutive material model '3D Non-Linear Cem. User' could be adopted to replicate the behavior of stone masonry or lime mortar for more refined results.

## 9. REFERENCES

1. Zucchini A, Lourenço PB. Mechanics of masonry in compression: Results from a homogenisation approach. *Computers & Structures*. 2007;85(3):193-204.
2. Ministry of Foreign Affairs of the Czech Republic Welcome to the Czech Republic: mzv.cz; 2011 [Available from: [https://www.mzv.cz/public/d3/8c/fb/740362\\_646055\\_Welcome\\_to\\_the\\_Czech\\_Rep.\\_2011.pdf](https://www.mzv.cz/public/d3/8c/fb/740362_646055_Welcome_to_the_Czech_Rep._2011.pdf)].
3. UNESCO. Baroque World Heritage 2020 [Available from: <https://whc.unesco.org/en/list/?search=baroque&order=country>].
4. Region Broumovsko 2020 [Broumov Region]. Available from: <https://www.broumovsko.cz/>.
5. Kulkarni Shantanu. Broumov Churches 2020 [Google Maps Location of List of Churches]. Available from: <https://goo.gl/maps/pRuaoYaV3gkAuX5PA>.
6. NAKI Project. Stones, sandpits and limestone quarries in the Czech Republic 2015 [Applied research and development of national and cultural identity ]. Available from: <http://kamenolomy.fzp.ujep.cz/eng/index.php?page=project>.
7. British Standard. BS EN 1926-1:1999. Natural Stone test methods- Determination of uniaxial compressive strength: BSI; 2006.
8. European Standard. EN 12372:2006 Natural stone test methods - Determination of Flexural strength under concentrated load: CEN/TC 246; 2006.
9. Kočí V, Maděra J, et. al. Service Life Assessment of Historical Building Envelopes Constructed Using Different Types of Sandstone: A Computational Analysis Based on Experimental Input Data. *The Scientific World Journal*. 2014;2014:802509.
10. Lourenco P, Zucchini A, et. al. Homogenization Approaches for Structural Analysis of Masonry Buildings. In: Lourenco PB, editor. SAHC 2006; New Delhi, India: Structural Analysis of Historical Construction; 2006.
11. Lourenco P. Masonry Modeling. 2015. p. 1419-31.

12. Lourenco P, Rots J. Multisurface Interface Model for Analysis of Masonry Structures. *Journal of Engineering Mechanics*. 1997;123:660-8.
13. Zhang X, Chen Z, Liu Y. Chapter 6 - Constitutive Models. In: Zhang X, Chen Z, Liu Y, editors. *The Material Point Method*. Oxford: Academic Press; 2017. p. 175-219.
14. Cervenka Consulting. *Atena Program Documentation Part 2-1*. 5 ed. Prague2015. p. User's Manual for Atena 2D.
15. Cervenka Consulting. *Atena Program Documentation Part 1 Theory*. Prague: Vladimir Červenka , Libor Jendele, Jan Červenka; 2018. p. This manual contains a detailed description about the theories used in ATENA software. The manual contains the description of finite elements, material models and nonlinear solution strategies.
16. British Standard. BS EN 1052-1:1999. *Methods of test for masonry Part 1- Determination of compressive strength*: BSI; 1999.
17. ASTM International. E519/E519M-15. *Standard Test Method for Diagonal Tension (Shear) in Masonry Assemblages*2015.
18. ASTM International. ASTM C1531-02. *Standard test method for insitu measurement of masonry mortar joint shear strength index*2002.
19. Borri A, Corradi M, et al. A method for the analysis and classification of historic masonry. *Bulletin of Earthquake Engineering*. 2015;13.
20. Gajjar Pratik. *Nonlinear numerical evaluations of the wall bearing capacity and the structure stability of the St Ann church from the broumov group of churches [Advanced masters]*: CZECH TECHNICAL UNIVERSITY IN PRAGUE; 2018.
21. Adamek John. *Stochastic Micro-modelling of Historic Masonry [Advanced Masters]*: Czech Technical University in Prague; 2019.



## **APPENDIX A- BROUMOV CHURCHES**

This page is left blank on purpose.

### Church of St. Jakub Větší in Ruprechtice:



Figure A1– Church of St Jakub Větší in Ruprechtice

<b>Address</b>	549 73 Martínkovice
<b>Timeline of construction</b>	1720-1723
<b>Chief Architect</b>	Kryštof Dientzenhofer

### Church of St. George and Martin in Martínkovice:



Figure A2– Church of St. George and Martin in Martínkovice

<b>Address</b>	549 73 Martínkovice
<b>Timeline of construction</b>	1690-1693
<b>Chief Architect</b>	Martin Allio

## Church of St. Anne in Vižňov



Figure A3– Church of St. Anne in Vižňov

<b>Address</b>	Vižňov, 549 83 Meziměstí
<b>Timeline of construction</b>	1719-1728
<b>Chief Architect</b>	Kilián Ignác Dientzenhofer

### Church of St. Michal in Verněřovice



Figure A4– Church of St. Michal in Verněřovice

<b>Address</b>	549 82 Verněřovice
<b>Timeline of construction</b>	1719-1722
<b>Chief Architect</b>	Kryštof Dientzenhofer

## Church of All Saints in Heřmánkovice



Figure A5– Church of All Saints in Heřmánkovice

<b>Address</b>	549 84 Heřmánkovice
<b>Timeline of construction</b>	1722-1724
<b>Chief Architect</b>	Kilián Ignác Dientzenhofer

## Church of St. Prokop in Bezděkov



Figure A6– Church of All Saints in Heřmánkovice

<b>Address</b>	Bezděkov nad Metují 69, 549 64 Bezděkov nad Metují
<b>Timeline of construction</b>	1724-1727
<b>Chief Architect</b>	Kilián Ignác Dientzenhofer



## Church of St. Barbora in Otovice



Figure A7– Church of St. Barbora in Otovice

<b>Address</b>	549 72 Otovice
<b>Timeline of construction</b>	1725-1727
<b>Chief Architect</b>	Kryštof Dientzenhofer

## Church of St. Margaret in Šonov



Figure A8– Church of St. St. Margaret in Šonov

<b>Address</b>	549 71 Šonov
<b>Timeline of construction</b>	1725-1727
<b>Chief Architect</b>	Kilián Ignác Dientzenhofer

## Church of St. Mary Magdalene in Božanov



Figure A9– Church of St. Mary Magdalene in Božanov

<b>Address</b>	549 74 Božanov
<b>Timeline of construction</b>	1735-1743
<b>Chief Architect</b>	Kilián Ignác Dientzenhofer

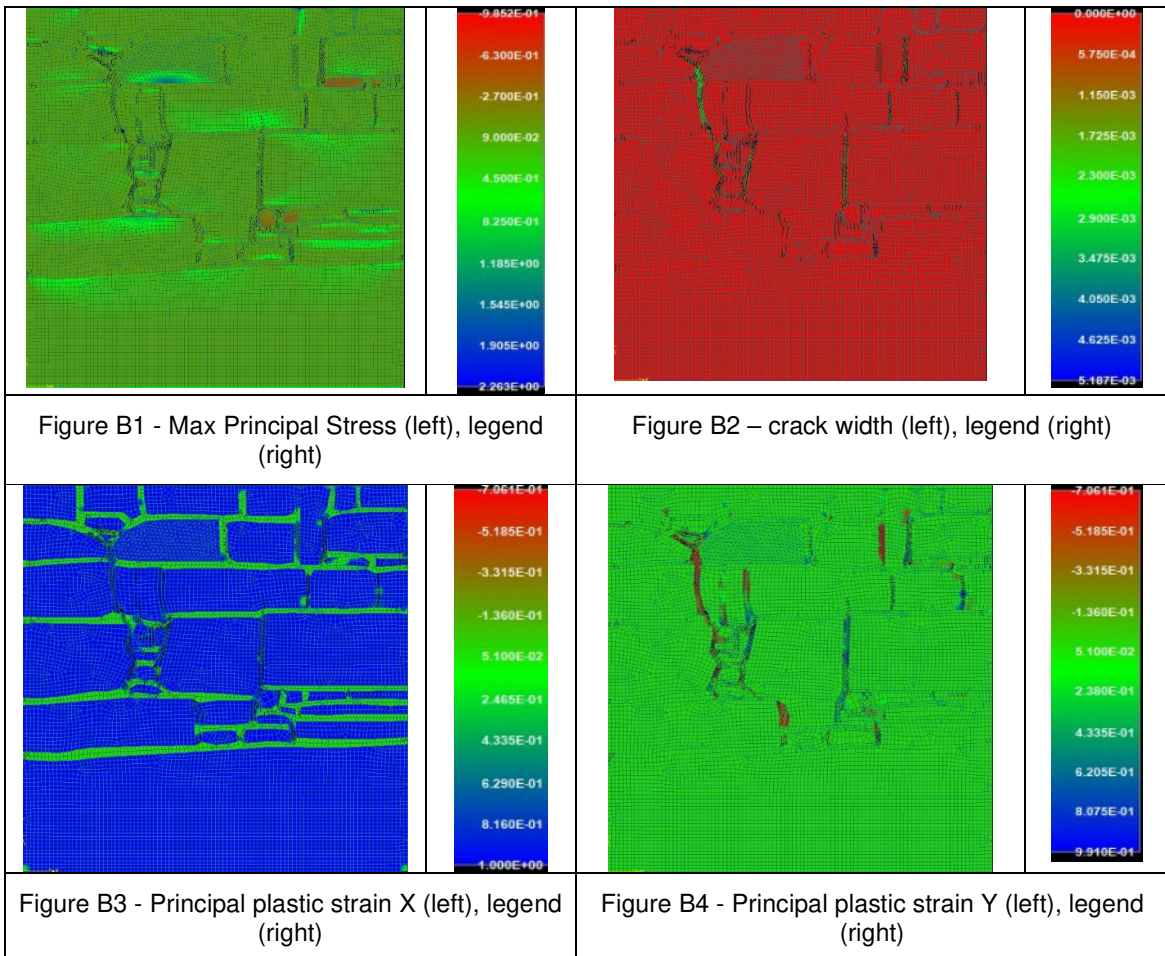
This page is left blank on purpose.

## **APPENDIX B- MODEL RESULTS**

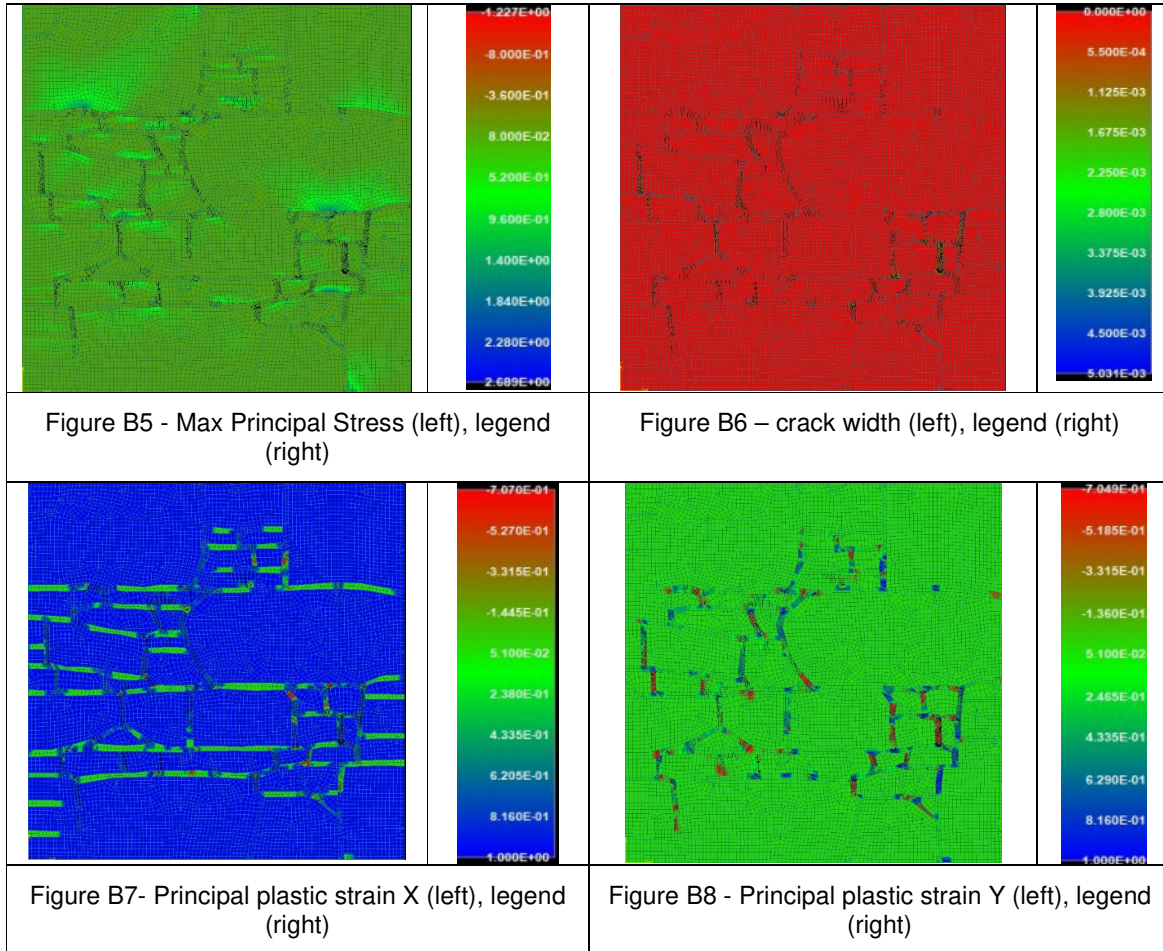
This page is left blank on purpose.

## COMPRESSION TEST

### Wall Assembly 1

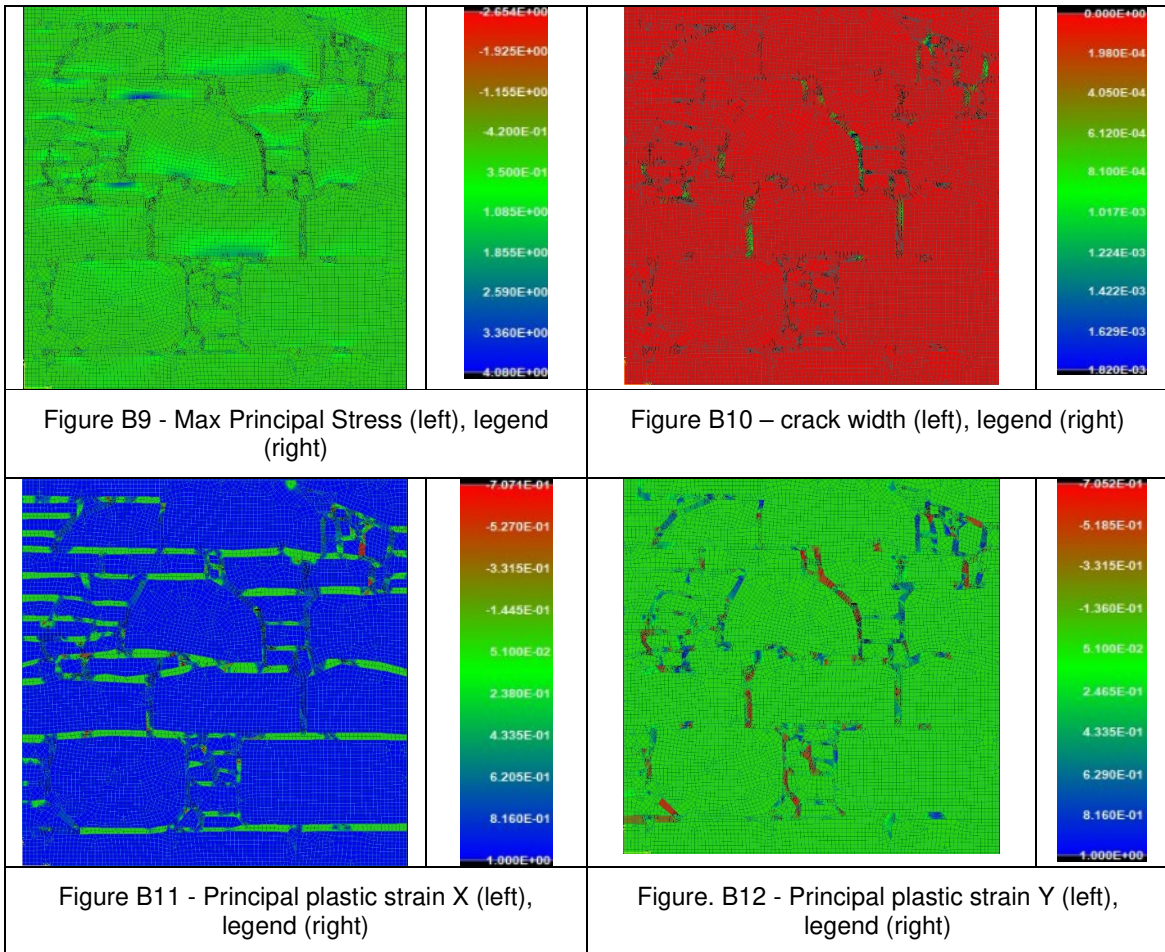


## Wall Assembly 2

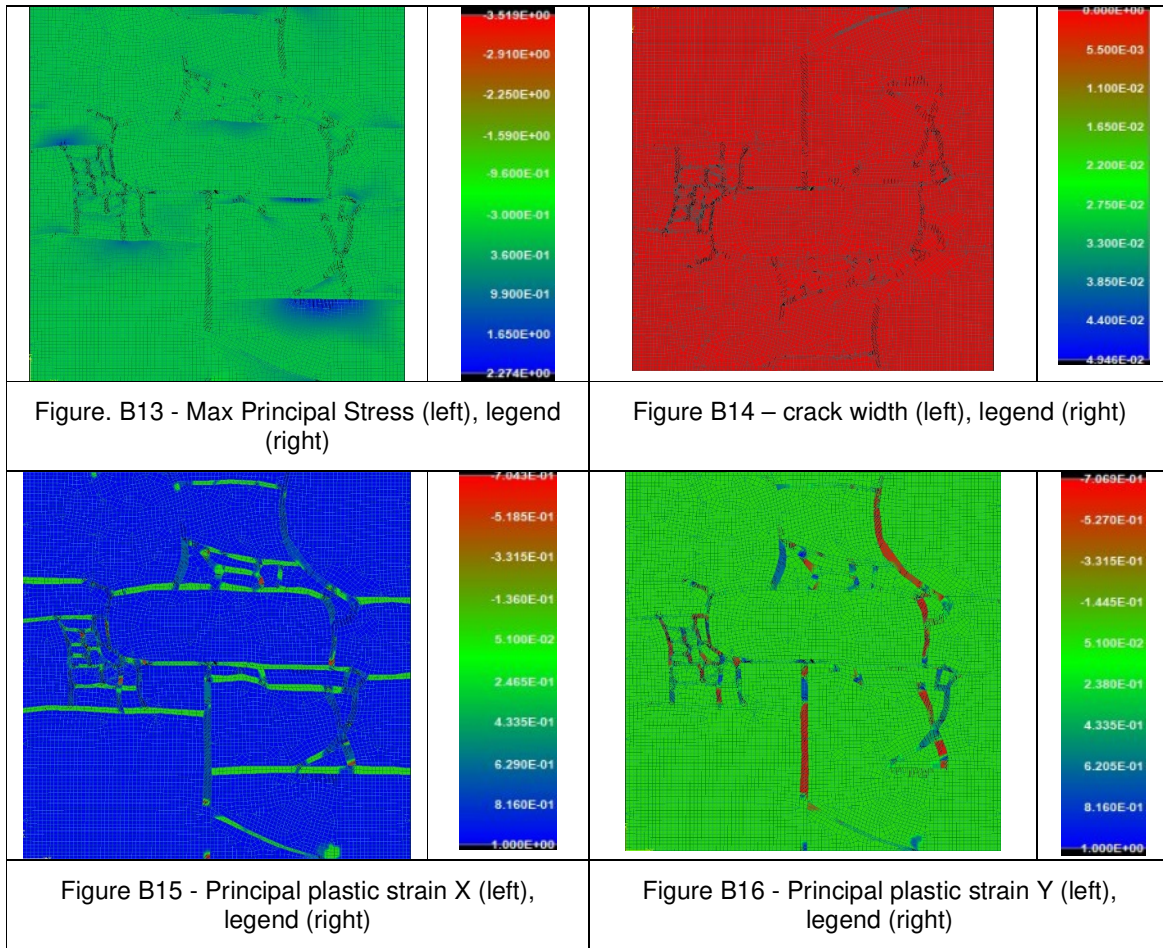




### Wall Assembly 3

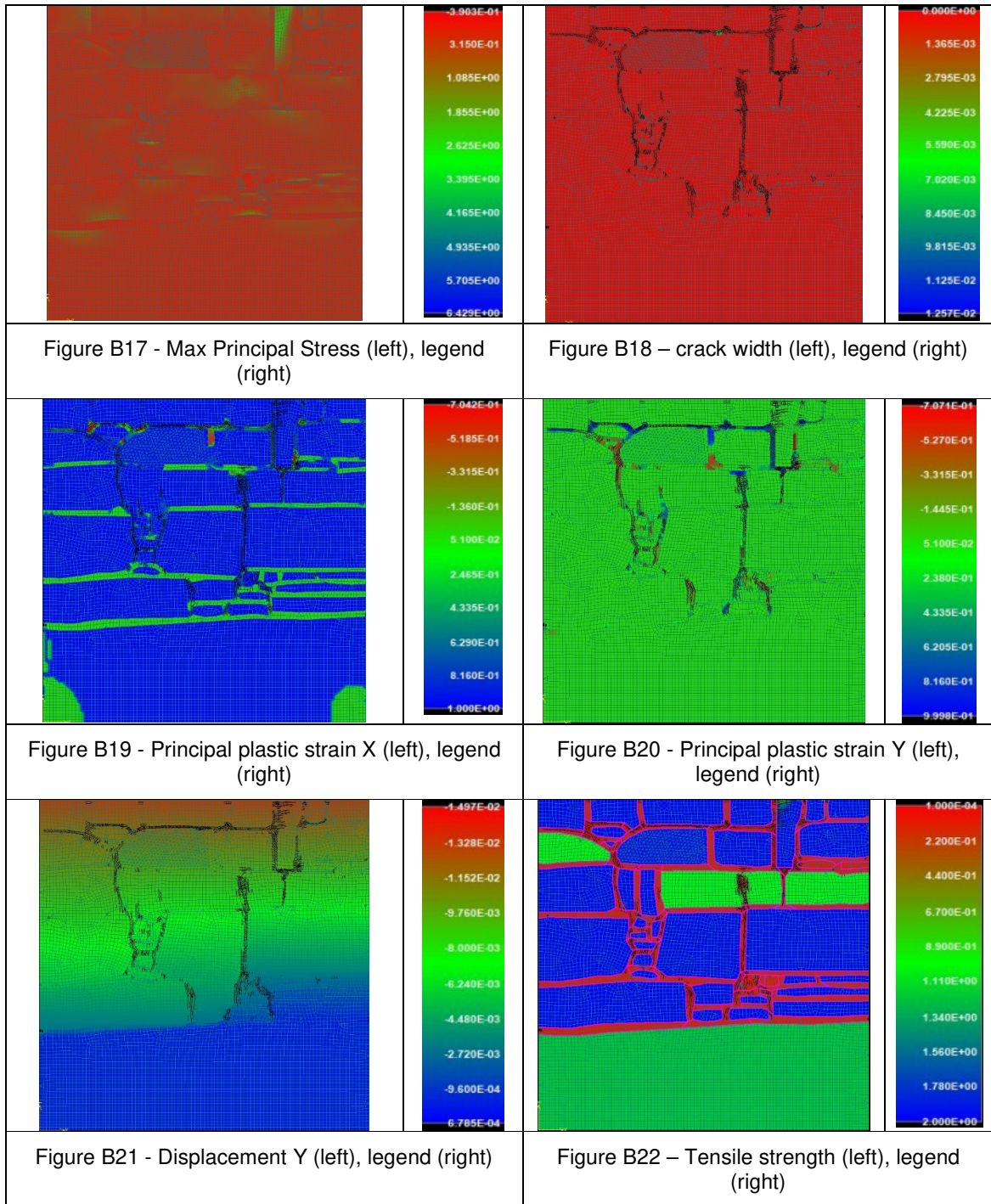


### Wall Assembly 4

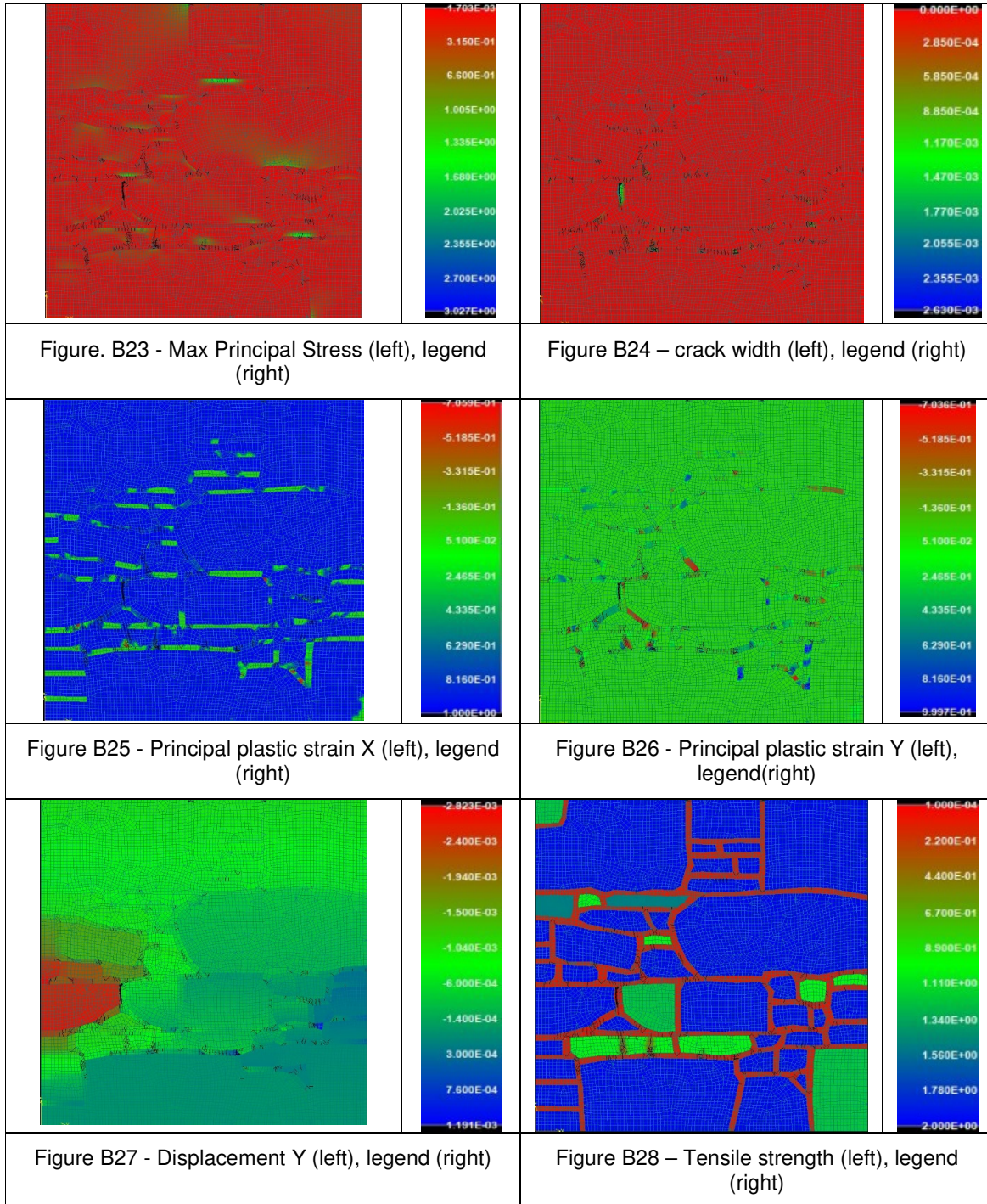


## TENSION TEST

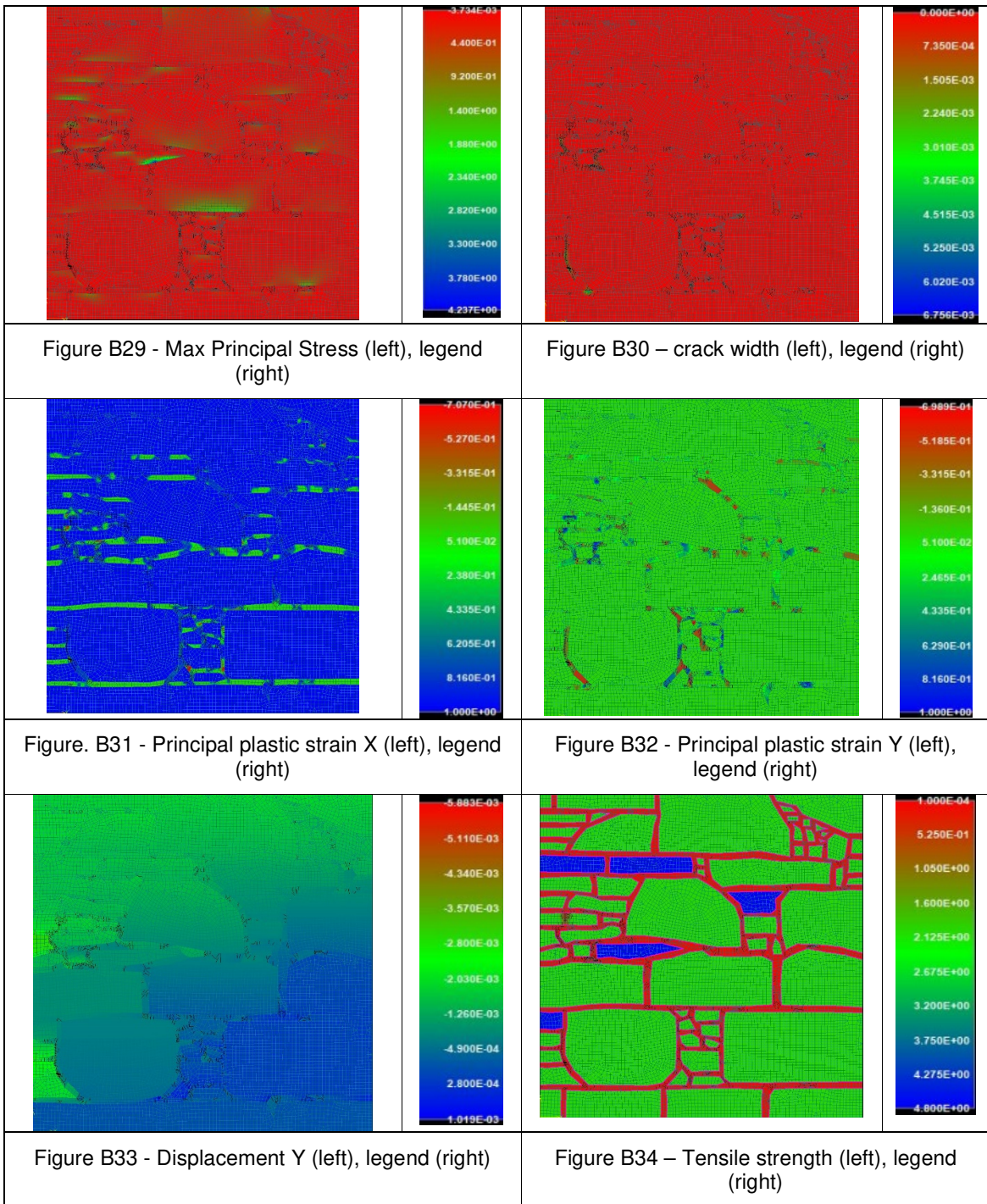
### Wall Assembly 1



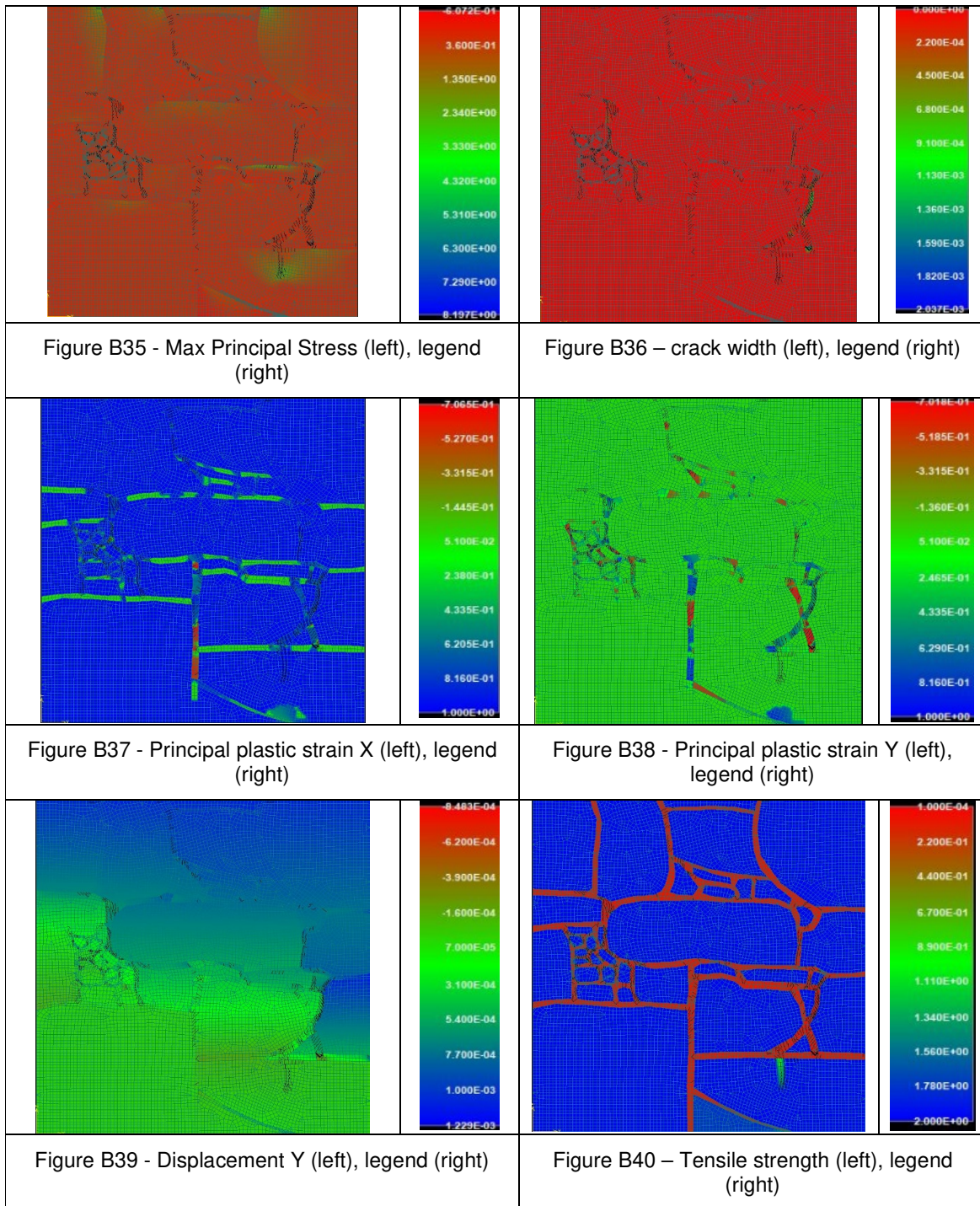
## Wall Assembly 2



### Wall Assembly 3

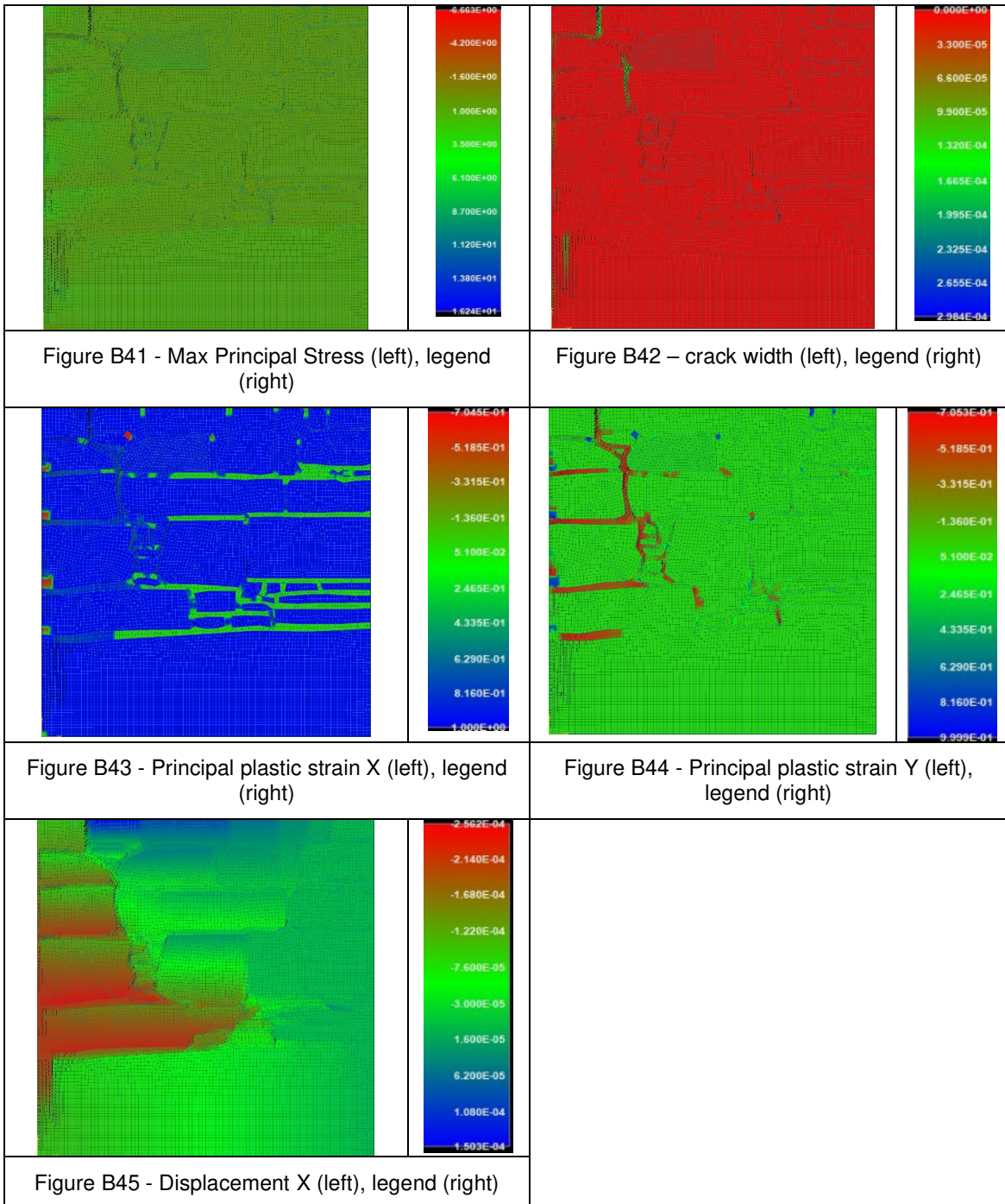


### Wall Assembly 4

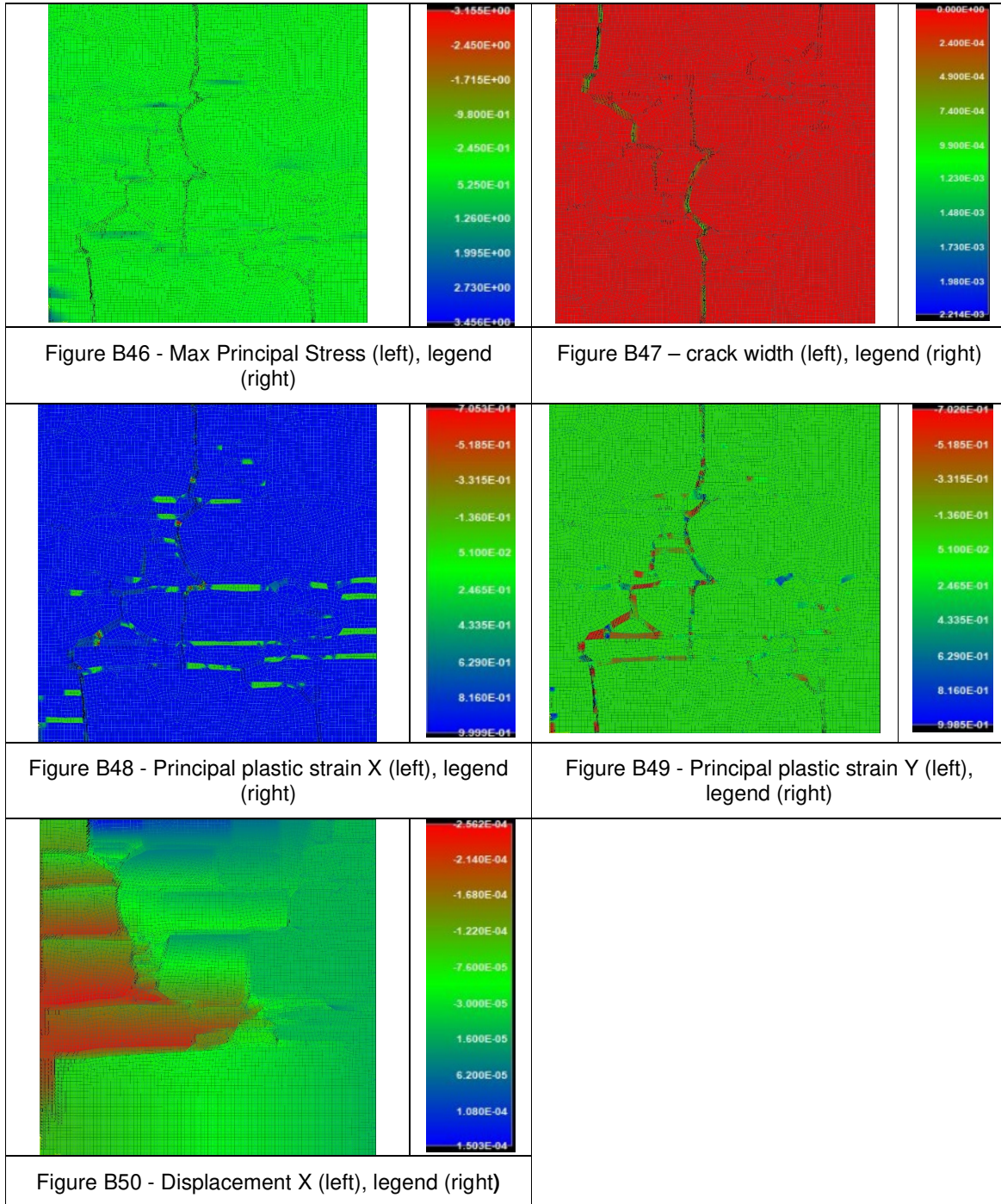


## SHEAR TEST

### Wall Assembly 1

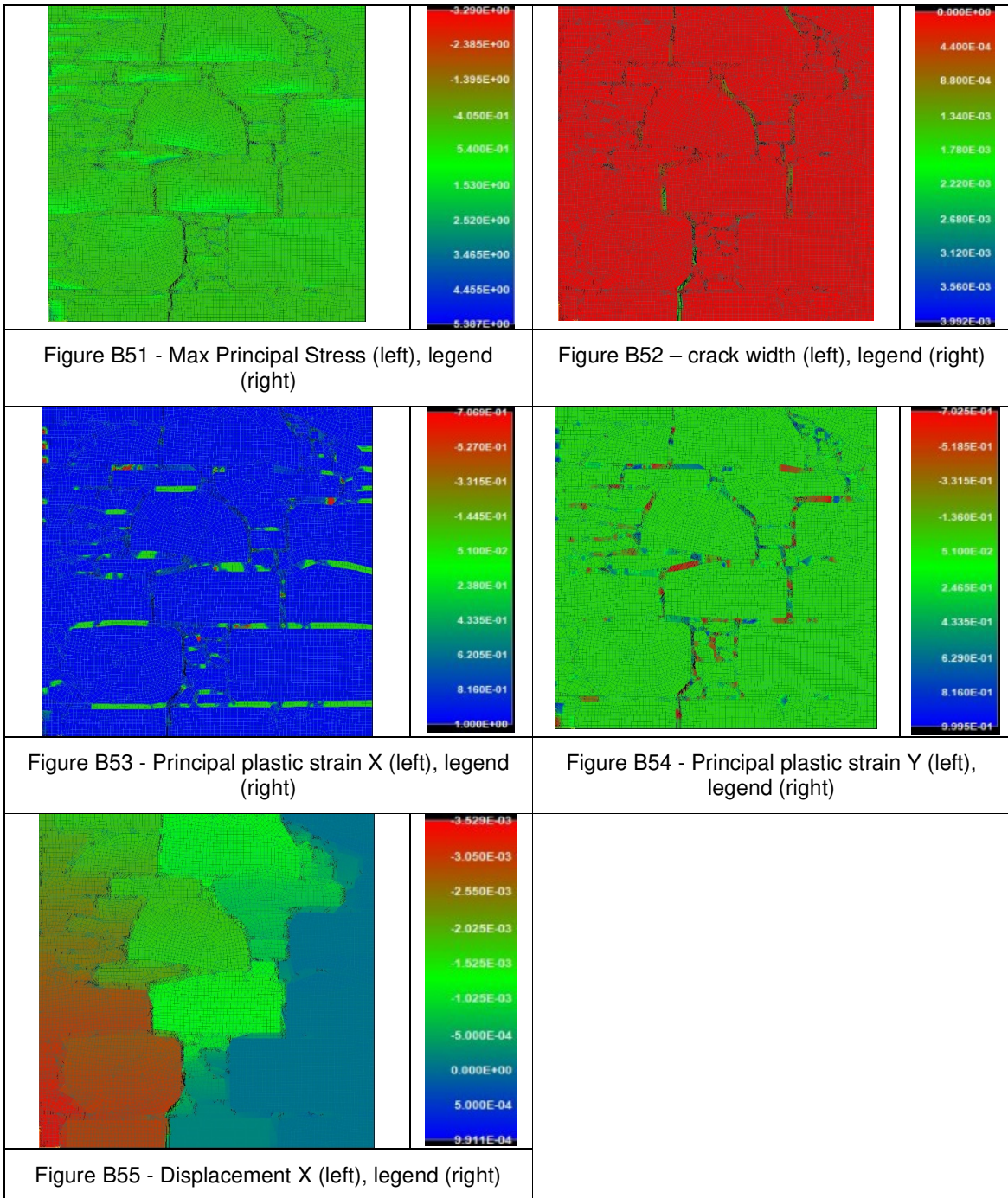


## Wall Assembly 2





### Wall Assembly 3



### Wall Assembly 4

